

Devonian integrative stratigraphy and timescale of China

Wenkun QIE^{1*}, Xueping MA², Honghe XU³, Li QIAO¹, Kun LIANG¹, Wen GUO⁴,
Junjun SONG⁴, Bo CHEN³ & Jianfeng LU⁴

¹ CAS Key Laboratory of Economic Stratigraphy and Palaeogeography, Nanjing Institute of Geology and Palaeontology and Center for Excellence in Life and Palaeoenvironment, Chinese Academy of Sciences, Nanjing 210008, China;

² School of Earth and Space Sciences, Peking University, Beijing 100871, China;

³ State Key Laboratory of Palaeobiology and Stratigraphy, Nanjing Institute of Geology and Palaeontology and Center for Excellence in Life and Palaeoenvironment, Chinese Academy of Sciences, Nanjing 210008, China;

⁴ Nanjing Institute of Geology and Palaeontology and Center for Excellence in Life and Palaeoenvironment, Chinese Academy of Sciences, Nanjing 210008, China

Received November 13, 2017; revised March 22, 2018; accepted August 13, 2018; published online October 12, 2018

Abstract The Global Boundary Stratotype Sections and Points (GSSPs) for the bases of all seven international Devonian stages have been formally defined and ratified by IUGS till 1996, and nowadays, the main tasks for Devonian stratigraphers include further subdivision of these standard stages, strictly constrained absolute ages for the boundaries, and precise neritic-pelagic and marine-terrestrial correlations using multidisciplinary stratigraphy methods. Establishment of high-resolution Devonian integrative stratigraphy framework and timescale of China would play an important role in improving regional and international correlation, facilitating the recognition of important stratigraphic levels in different paleogeographic settings, and understanding the evolution pattern of biota, paleoclimate and palaeoenvironment during this critical interval. Based on well-studied bio- and chronostratigraphy of Devonian in South China and adjacent areas, in combination with recent achievements in carbon isotope stratigraphy, event stratigraphy and radioactive isotope ages, this paper briefly summarize the research history and current status of Devonian chronostratigraphy of China, and for the first time introduce Devonian integrative stratigraphy framework of China. Up to date, few studies have been conducted on the astronomical cyclostratigraphy and high-resolution radioactive isotope dating in Devonian of China, which should be our main focuses in the near future.

Keywords Devonian, Chronostratigraphy, Biostratigraphy, Carbon isotope stratigraphy, Event stratigraphy

Citation: Qie W K, Ma X P, Xu H H, Qiao L, Liang K, Guo W, Song J J, Chen B, Lu J F. 2019. Devonian integrative stratigraphy and timescale of China. *Science China Earth Sciences*, 62: 112–134, <https://doi.org/10.1007/s11430-017-9259-9>

1. Introduction

The Devonian (419.2–358.9 Ma) is the first geological period of the late Paleozoic, spanning about 60.3 Ma from the end of the Silurian, and its beginning is marked by the First Appearance Datum (FAD) of graptolite *Uncinatograptus uniformis* (Přibyl, 1940) (Gradstein et al., 2012).

During this time interval, the Earth's climate system un-

derwent severe perturbations, characterized by drastic dropdown of atmospheric CO₂ concentration, multiple cooling events, and gradual transition from the Silurian 'greenhouse' Earth to the Permo-Carboniferous 'icehouse' Earth (Joachimski et al., 2009; Foster et al., 2017). The complex pattern of climate change during the Devonian were controlled by multiple factors at different time scales. On longer time scale (millions to tens of millions of years), ocean-continent configuration, tectonic activity and terrestrial flora evolution were the most important factors (Algeo

* Correspondence author (email: wkqie@nigpas.ac.cn)

et al., 1995; Godd ris et al., 2014), while on short time scale (tens to hundreds of thousands of years), Earth orbit variation was considered as the main dynamic controlling Earth's climate system, which in turn, exert a major impact on biota evolution (De Vleeschouwer et al., 2013). However, the lack of precise stratigraphic subdivision and correlation in different paleogeographic settings, which was mainly caused by predominantly endemic fauna and flora and commonly discontinuous successions in the neritic and terrestrial facies, causes the biodiversity variation pattern, biota evolutionary process and their relationships to the climatic and environmental events unclear (Racki, 2005; Kaiser et al., 2016). Therefore, establishment of high-resolution Devonian integrative stratigraphy and timescale framework is essential for the studies on the complex ocean-land-atmosphere interactions during Devonian at different temporal and spatial scales.

The term 'Devonian' was first proposed by Sedgwick and Murchison (1839), to define the marine rocks in Devon, southwest England, which were considered to be the equivalents of terrestrial Old Red Sandstone deposits in Wales. In 1985, the global Devonian chronostratigraphy

scale was formally defined and subdivided into three series, the lower, middle and upper, and contains seven global stages (Ziegler and Klapper, 1985). The lower Devonian comprises the Lochkovian, Pragian and Emsian stages in ascending order, the middle Devonian consists of the Eifelian and Givetian, and the upper Devonian comprises the Frasian and the ensuing Famennian (Table 1). Ratified by IUGS in 1972, the basal Devonian GSSP is the first 'golden spike' established by the International Commission on Stratigraphy (Chlup c and Kukal, 1977). Till 1996, all seven Devonian stages' GSSPs have been formally defined and ratified (Yolkin et al., 1997). It should be noted though, that the acceptance of the GSSPs for the bases of the Emsian and the Devonian-Carboniferous boundary (DCB) have received major criticism since the very beginning of their ratification, and in 2008, the Subcommittee on Devonian Stratigraphy (SDS) and Subcommittee on Carboniferous Stratigraphy (SCCS) have decided to redefine the boundary criteria and levels (Becker, 2009; Aretz, 2010), which are still ongoing investigations (Slav k and Brett, 2016; Spalletta et al., 2017; Table 1).

In China, there are numerous well-preserved Devonian

Table 1 Global and Chinese correlation chart of Devonian chronostratigraphic units^{a)}

Global chronostratigraphy					Chinese regional chronostratigraphy			
Series	Stage	Sub-stage	Boundary definition	GSSP location	Ratified by IUGS	Stage	Unit stratotype definition	Reference section
Upper	Tou.		FAD <i>S. sulcata</i> (C)	base of Bed 89 in Trench E' La Serre, France	1990	Tournaisian		
	Famennian		FAD <i>Pr. kockli</i> ?	Base of Bed 32a in Coumiac Quarry, France	1993	Shaodongian	FAD <i>Eoendothyra regularis</i> (F)	Huilong, Guilin
			FAD <i>Pa. triangularis</i> (C)			Yangshuoan	FAD <i>Palmatolepis r. trachytera</i> (C)	Tieshan, Guilin, Guangxi
	Frasnian			Base of Bed 42 in Col du Poech de La Suque E Montagne Noire, France	1987	Xikuangshanian	<i>Cyrtiopsis-Yunnanella-Sinospirifer</i> (B)	Xikuangshan, Lengshuijiang, Hunan
		FAD <i>A. r. pristina</i> (C)		Shetianqiaoan		F-F mass extinction event		Shetianqiao, Shaodong, Hunan
Middle	Givetian		Base of Bed 123 in Jebel Mech Irdane, Morocco	1994	Dongganglingian	<i>Sunophyllum-Endophyllum-Trunci.</i> (Cor)	Ma'an'shan, Xiangzhou, Guangxi	
		FAD <i>P. hemiansatus</i> (C)				<i>Nowakia otomari</i> (T)		
Lower	Eifelian		Base of Wp30 in Wetteldorf, Eifel Hills, Germany	1985	Yingtangian	<i>Xenospirifer tongi-Eospiriferina lachrymosa</i>	Dale, Xiangzhou, Guangxi	
		FAD <i>P. c. partitus</i> (C)				<i>-Yingtangella sulcatilis</i> (B)		
	Emsian		Base of Bed 9/ 5, Zinzilban Gorge, Uzbekistan	1996	Sipaian		Ertang(Wuxuan)-Dale(Xiangzhou), Guangxi	
		FAD <i>P. excavatus</i> 114? FAD <i>P. kitabicus</i> (C)				FAD <i>Erbenoceras</i> etc.(A)		
Pragian		Base of Bed 12, in Velka Chuchle, Czech Republic	1989	Yujiangian	<i>R. tonkinensis-Dicoelostrophia</i> (B)	Liujiang, Hengxian, Guangxi		
		FAD <i>E. s. sulcatus</i> (C)		Nagaolingian	<i>Orientospirifer nakaolingensis</i> (B)	Liujiang, Hengxian, Guangxi		
Lochkovian		Base of Bed 20, in Klonek near Prague, Czech Republic	1972	Lianhuashanian	<i>Zosterophyllum-Uncatoella verticillata</i> (P) <i>Polybranchiaspis-Yunnanolepis</i> (Fi)	Xishancun, Qujing Yunnan		
		FAD <i>U. uniformis</i> (G)			FAD <i>P. scitulus,P.trilobutus,P.cornuformis</i> (V)			

a) Modified after unpublished report of Hou et al. (2011), the stratigraphic chart of China (2014) and the Geological Time Scale 2016. A = Ammonite, B = Brachiopod, C = Conodont, Cor = Coral, G = Graptolite, T = Tentaculite, F = Foraminifer, Fi = Fish, V = Vertebrate.

stratigraphic successions formed in different paleoplates, recording a variety of lithofacies and biofacies. Detailed studies of diverse fossil groups in the nearly complete marine sequences in South China make it an ideal area for the further improvement of Devonian chronostratigraphy scale. The pioneering reports on the Devonian fossils in China were published by De Koninck (1846) and Davidson (1853) in the middle 19th century, to describe a few brachiopods from South China, and recently, the Stratigraphic Chart of China (2014) has been officially issued by the National Commission on Stratigraphy of China, refining the Devonian regional chronostratigraphy scale and enabling precise correlation between the Chinese and international chronostratigraphy. Nevertheless, there are still many deficiencies concerning the Chinese Devonian stages, including (1) lack of strict definition for the boundaries of the Chinese regional stages, which are defined by unit-stratotypes rather than boundary stratotype, there might be overlap/or gap between the neighboring units; (2) most unit-stratotypes of the Chinese regional stages are established in shallow-water platform facies, characterized by low-resolution biozonations (e.g., rugose coral, brachiopod biozones) and poor correlation with other regions; (3) lack of systematic, integrative studies on the event stratigraphy, chemostratigraphy and absolute age dating in the stratotype sections and of further subdivision of the regional stages. This paper aims to briefly summarize the research history, current status and achievement of Devonian chronostratigraphy of China, to provide an updated Devonian integrative stratigraphy framework of China, and to propose the future research fields.

2. History and subdivision of Devonian chronostratigraphy of China

In China, Devonian-related studies have lasted for about 170 years, it started with sparse fossil descriptions and geological routine investigations in the middle 19th century, and significant palaeontological and stratigraphic works were carried out in the 1930s (Feng, 1930; Grabau, 1931; Yoh, 1938). Tien (1938) summarized previous Devonian studies in South China, in combination with new collections from several type sections in Yunnan, Guangxi and Hunan, first subdivided the Devonian of China into lower, middle and upper series, consisting of 11 standard beds (Table 2). On the basis of Tien's subdivision, Wang and Yu (1962) proposed to establish six Chinese regional stages, including the Longhuashanian, Sipaian/or Nagaolingian stages of the lower Devonian, the Yujiangian and Dongganglingian stages of the middle Devonian and the Shetianqiaoan and Xikuangshanian stages of the upper Devonian (Table 2). During this time, the subdivision of Devonian in China was

mainly based on the stratigraphic distributions of benthic fauna (e.g., brachiopods and rugose corals) in South China.

Since the 1970s, important Devonian fossil groups which are biostratigraphically significant, including conodont, ammonite, graptolite and tentaculite, have been constantly reported in China and the biostratigraphic sequences in pelagic facies have been preliminarily established (Ruan, 1979; Bai et al., 1982; Ruan and Mu, 1989; Mu et al., 1988, Wang, 1989). Major progresses has been made regarding international correlation and recognition of important chronostratigraphic boundaries (Wang et al., 1981; Yu, 1988), manifested by the establishment of the International Auxiliary Stratotype Section of the Devonian-Carboniferous boundary near Nanbiancun in Guilin (Paproth et al., 1991). Based on the new advances in biostratigraphy in pelagic facies, Wang et al. (1974), Hou (1978) and Hou et al. (1988) revised previous Devonian chronostratigraphic division of China: (1) replacing the Longhuashanian Stage with the Lianhuashanian Stage; (2) placing the Yujiangian Stage as the third stage of the lower Devonian; (3) assigning the Sipaian to the uppermost lower Devonian; (4) establishing a new chronostratigraphic units, the Yingtangian Stage, to represent the lower part of the middle Devonian. This division has been widely accepted till the early 21th century (Table 2).

From the 1990s to present, Chinese scholars conducted significant studies on chemostratigraphy, event stratigraphy, cyclostratigraphy and radioactive isotope dating (Bai et al., 1994; Chen et al., 2005; Gong et al., 2005; Liu et al., 2012; Chang et al., 2017) while kept refining the biostratigraphic sequences of Devonian, with the intention of making accurate stratigraphy correlation between different regions using multidisciplinary methods. However, most achievements are constrained within 3–4 conodont biozones around the key stage boundaries, such as Givetian-Frasnian and Frasnian-Famennian boundaries. During this period, Hou and Ma (2005) redefine the Shaodongian Stage as the topmost Devonian of China, with its base marked by the FAD of foraminifer *Eoendothyra regularis*. The Yangshuoan Stage, consistent with the middle and upper Famennian, was recently established by the National Commission on Stratigraphy of China and characterized by the FAD of conodont *Palmatolepis rugosa trachytera* (Table 1). Since the Devonian units of the standard global chronostratigraphic scale have been formally defined in 1985, some Chinese Devonian stratigraphers propose to adopt the global standard stages and abandon the Chinese regional stages, while others claimed that the standard global chronostratigraphic scale is valid only as it is based on sound, detailed regional stratigraphy, and the units of regional chronostratigraphy will always be needed (Hou et al., 1988; Liao and Ruan, 2003; Hou and Ma, 2005; Wang and Peng, 2017)(Table 2).

Table 2 Historical subdivision of the Devonian System in China^{a)}

Tien (1938)			Wang and Yu (1962)		Hou (1978)	Hou et al. (1988)	Zhong et al. (1992) Wang and Peng (2017)	Hou and Ma (2005)		NCSC (2014)									
Upper (Hunan Series)	KKS Group	Magunao limestone	Upper (Hunan Series)	Xikuangshanian	Upper Series	Xikuangshanian	Upper Series	Famennian	Upper Series	Shaodongian	Upper Series	Shaodongian							
		Tuzitang limestone								'unknown'		Yangshuoan							
	Shetian-qiao lime.	Shetianqiaoan								Shetianqiaoan		Frasnian	Shetianqiaoan	Shetianqiaoan	Shetianqiaoan	Shetianqiaoan			
Longkou-chong Bed	Donggang-lingian		Donggang-lingian	Givetian	Donggang-lingian	Donggang-lingian													
Middle (Guangxi Se.)		DS Group					JWZ lime. SJQ Bed JP limestone	Middle (Guangxi Series)	Yujiangian	Middle Series	Donggang-lingian	Middle Series	Givetian	Middle Series	Donggang-lingian	Middle Series	Donggang-lingian		
	XX Group	Bangzhai sandstone Wucun shale	Yujiangian	Yingtangian	Eifelian	Yingtangian	Yingtangian												
Lower (Xiuren Series)	Sipai shale	Sipai shale						Middle (Guangxi Series)	Yujiangian	Lower Series	Sipaian	Lower Series	Emsian	Lower Series	Sipaian	Lower Series	Sipaian		
			Longhuashan sandstone	Longhuashanian	Yujiang	Yujiangian	Pragian											Yujiangian	Yujiangian
	Lower (Yunnan Series)	Longhuashanian	Lianhuashanian	Lower Series	Lochkovian	'unknown'	Lianhuashanian												

a) XKS = Xikuangshan, STQ = Shetianqiao, DS = Dushan, XX = Xiangxian, JWZ = Jiwozhai, SJQ = Songjiaqiao, JP = Jipao.

3. Devonian integrative stratigraphy framework of China

The Devonian chronostratigraphic study aims to establish precise stratigraphic framework of the period between 419.2 Ma and 358.9 Ma, and enable the global correlation among different paleogeographic settings. The resolution of the existing Devonian geological time scale, established by biostratigraphic researches and radiometric ages, is relatively low and sometimes with a ± 6 Myr uncertainty (Becker et al., 2012) (Figure 1), which is insufficient for the study of Devonian biotic and paleoenvironmental events with duration of tens to hundreds of thousands of years (De Vleeschouwer et al., 2013; Myrow et al., 2013). Thus, based on biostratigraphic evidences and absolute age constraints, a higher-resolution stratigraphic framework is needed and should be generated through integrated studies of chemostratigraphy, cyclostratigraphy, and quantitative stratigraphy. In addition, recognizing the Milankovitch Cycles in Devonian successions through paleoclimate indicators, and precisely timing

the geological boundaries and events by astronomical tuning are also increasingly valued. In this paper, we intend to summarize the achievements in type sections of Devonian in South China and adjacent regions, and provide an updated integrated stratigraphic framework (Figures 1–3).

3.1 Devonian biostratigraphy of China

Devonian chronostratigraphic division and correlation are mainly based on biostratigraphy studies. In China, biostratigraphic sequences of major fossil groups have been elaborately summarized by Wang (2000), Cai (2000), Liao and Ruan (2003), and are presented herein in Figures 1 and 2. Recent advances in biostratigraphic research of conodonts, graptolites, ostracods, brachiopods, rugose corals, as well as spores and plants are emphatically introduced in this paper.

3.1.1 Conodont

Conodont is a key taxon in the Devonian biostratigraphic research. 6 out of the 7 global stages of Devonian, except for

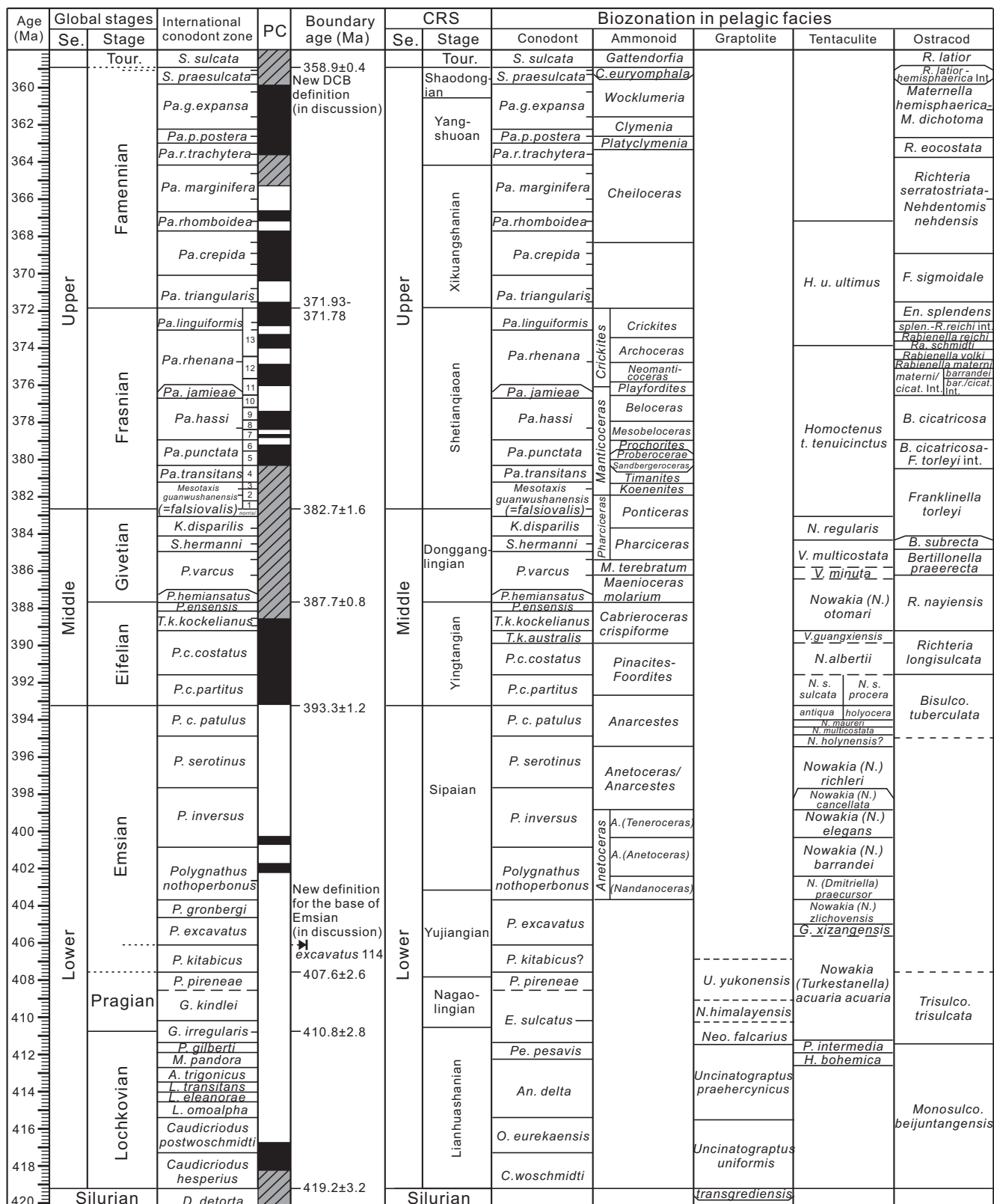


Figure 1 Devonian Chronostratigraphy and biozonations in pelagic facies in China. International standard chronostratigraphy units, conodont zones and absolute ages are after Becker et al. (2012) and Percival et al. (2018); Polarity Chron is after Becker et al. (2012) and Ogg (2016); Chinese regional chronostratigraphy units (CRS) are after the stratigraphic chart of China (2014); Devonian biozonations of important fossil groups in China, including the conodont, ammonite, graptolite and ostracod, are after Wang (2018), Liao and Ruan (2003), Mu and Ni (1975) and Chen et al. (2015), Ruan and Mu (1989), Wang (2009), respectively.

Age (Ma)	Chronostratigraphy		Biozonation in shallow marine and non-marine facies									
	Se.	Stage	Regional stage	Brachiopod	Coral	Microvertebrate ^{a)}	Macrovertebrate	Chitinozoan ^{b)}	Sporepollen	Macroplants		
360	Upper	Tour.	Shao-dongian	Yan. dushanensis- Plico. ornatus- Trifi. longhuiensis	Cystophrentis Ceriphyllum	Acanthodes guizhouensis	Sinolepis	Cingulochitina sp.	le.-nitidus le.-explanatus R. lepidophyta- K. literatus R. lepidophyta- K. literatus	LN LE LL LV	Sublepidodendron- Shougangia- Hamatophyton	
362				Famennian	Yang-shuoan	Nayunnella- Hunanospirifer		Smithiphyllum	Phoebodus cf. Ph. limpidus	Remigolepis		Angochitina sp.
364		Xikuangshanian	Yunnanella- Sinospirifer				Dzieduszy					Acanthodes- Ctenacanthus
366				Frasnian	Shetianqiaocao	Cyrtospirifer		Peneckiella- Pseudozaphrentis	Phoebodus bifurcatus	Changyanophyton- Chirodipteris		
368		Donggang- lingian	"Leiorhynchus"				Stringocephalus					Sinodisphyllum
370				Eifelian	Yingtangian	Athyrisinga- Yingtangella- Xenospirifer		Utaratuia- Brevisseptophyllum	Dangdouichthys liui	Bothriolepis sinensis- Hunanolepis		
372		Emsian	Sipaian				Euryspirifer shujiapiensis Otospirifer shipaiensis Trigonospirifer trigonata					Zalimir Plectodonta
374				Yujiangian	Rostrospirifer tonkinensis- Dicoelostrophia	Sinaethyris		Lyriellasma- Xiangzhouphyllum	Wuxuanichthys wangi	Kueichowlepis- Sinopetalichthys		
376		Pragian	Nagao- lingian				Orientospirifer nakaolingensis					Chalcidophyllum- Eoglossophyllum
378				Lochkovian	Lianhuashanian	Spirigerina supermarginalis		Gomphonchus lujingensis	Cheiracanthoides wangi	Diabolepis- Nanpanaspis		
380	Lochkovian	Lianhuashanian	Spirigerina supermarginalis				Gomphonchus lujingensis				Cheiracanthoides dolosus	Diabolepis- Nanpanaspis
382				Lochkovian	Lianhuashanian	Spirigerina supermarginalis		Gomphonchus lujingensis	Cheiracanthoides dolosus	Diabolepis- Nanpanaspis		
384	Lochkovian	Lianhuashanian	Spirigerina supermarginalis				Gomphonchus lujingensis				Cheiracanthoides dolosus	Diabolepis- Nanpanaspis
386				Lochkovian	Lianhuashanian	Spirigerina supermarginalis		Gomphonchus lujingensis	Cheiracanthoides dolosus	Diabolepis- Nanpanaspis		
388	Lochkovian	Lianhuashanian	Spirigerina supermarginalis				Gomphonchus lujingensis				Cheiracanthoides dolosus	Diabolepis- Nanpanaspis
390				Lochkovian	Lianhuashanian	Spirigerina supermarginalis		Gomphonchus lujingensis	Cheiracanthoides dolosus	Diabolepis- Nanpanaspis		
392	Lochkovian	Lianhuashanian	Spirigerina supermarginalis				Gomphonchus lujingensis				Cheiracanthoides dolosus	Diabolepis- Nanpanaspis
394				Lochkovian	Lianhuashanian	Spirigerina supermarginalis		Gomphonchus lujingensis	Cheiracanthoides dolosus	Diabolepis- Nanpanaspis		
396	Lochkovian	Lianhuashanian	Spirigerina supermarginalis				Gomphonchus lujingensis				Cheiracanthoides dolosus	Diabolepis- Nanpanaspis
398				Lochkovian	Lianhuashanian	Spirigerina supermarginalis		Gomphonchus lujingensis	Cheiracanthoides dolosus	Diabolepis- Nanpanaspis		
400	Lochkovian	Lianhuashanian	Spirigerina supermarginalis				Gomphonchus lujingensis				Cheiracanthoides dolosus	Diabolepis- Nanpanaspis
402				Lochkovian	Lianhuashanian	Spirigerina supermarginalis		Gomphonchus lujingensis	Cheiracanthoides dolosus	Diabolepis- Nanpanaspis		
404	Lochkovian	Lianhuashanian	Spirigerina supermarginalis				Gomphonchus lujingensis				Cheiracanthoides dolosus	Diabolepis- Nanpanaspis
406				Lochkovian	Lianhuashanian	Spirigerina supermarginalis		Gomphonchus lujingensis	Cheiracanthoides dolosus	Diabolepis- Nanpanaspis		
408	Lochkovian	Lianhuashanian	Spirigerina supermarginalis				Gomphonchus lujingensis				Cheiracanthoides dolosus	Diabolepis- Nanpanaspis
410				Lochkovian	Lianhuashanian	Spirigerina supermarginalis		Gomphonchus lujingensis	Cheiracanthoides dolosus	Diabolepis- Nanpanaspis		
412	Lochkovian	Lianhuashanian	Spirigerina supermarginalis				Gomphonchus lujingensis				Cheiracanthoides dolosus	Diabolepis- Nanpanaspis
414				Lochkovian	Lianhuashanian	Spirigerina supermarginalis		Gomphonchus lujingensis	Cheiracanthoides dolosus	Diabolepis- Nanpanaspis		
416	Lochkovian	Lianhuashanian	Spirigerina supermarginalis				Gomphonchus lujingensis				Cheiracanthoides dolosus	Diabolepis- Nanpanaspis
418				Lochkovian	Lianhuashanian	Spirigerina supermarginalis		Gomphonchus lujingensis	Cheiracanthoides dolosus	Diabolepis- Nanpanaspis		
420	Lochkovian	Lianhuashanian	Spirigerina supermarginalis				Gomphonchus lujingensis				Cheiracanthoides dolosus	Diabolepis- Nanpanaspis
422				Lochkovian	Lianhuashanian	Spirigerina supermarginalis		Gomphonchus lujingensis	Cheiracanthoides dolosus	Diabolepis- Nanpanaspis		
424	Lochkovian	Lianhuashanian	Spirigerina supermarginalis				Gomphonchus lujingensis				Cheiracanthoides dolosus	Diabolepis- Nanpanaspis
426				Lochkovian	Lianhuashanian	Spirigerina supermarginalis		Gomphonchus lujingensis	Cheiracanthoides dolosus	Diabolepis- Nanpanaspis		
428	Lochkovian	Lianhuashanian	Spirigerina supermarginalis				Gomphonchus lujingensis				Cheiracanthoides dolosus	Diabolepis- Nanpanaspis
430				Lochkovian	Lianhuashanian	Spirigerina supermarginalis		Gomphonchus lujingensis	Cheiracanthoides dolosus	Diabolepis- Nanpanaspis		
432	Lochkovian	Lianhuashanian	Spirigerina supermarginalis				Gomphonchus lujingensis				Cheiracanthoides dolosus	Diabolepis- Nanpanaspis
434				Lochkovian	Lianhuashanian	Spirigerina supermarginalis		Gomphonchus lujingensis	Cheiracanthoides dolosus	Diabolepis- Nanpanaspis		
436	Lochkovian	Lianhuashanian	Spirigerina supermarginalis				Gomphonchus lujingensis				Cheiracanthoides dolosus	Diabolepis- Nanpanaspis
438				Lochkovian	Lianhuashanian	Spirigerina supermarginalis		Gomphonchus lujingensis	Cheiracanthoides dolosus	Diabolepis- Nanpanaspis		
440	Lochkovian	Lianhuashanian	Spirigerina supermarginalis				Gomphonchus lujingensis				Cheiracanthoides dolosus	Diabolepis- Nanpanaspis
442				Lochkovian	Lianhuashanian	Spirigerina supermarginalis		Gomphonchus lujingensis	Cheiracanthoides dolosus	Diabolepis- Nanpanaspis		
444	Lochkovian	Lianhuashanian	Spirigerina supermarginalis				Gomphonchus lujingensis				Cheiracanthoides dolosus	Diabolepis- Nanpanaspis
446				Lochkovian	Lianhuashanian	Spirigerina supermarginalis		Gomphonchus lujingensis	Cheiracanthoides dolosus	Diabolepis- Nanpanaspis		
448	Lochkovian	Lianhuashanian	Spirigerina supermarginalis				Gomphonchus lujingensis				Cheiracanthoides dolosus	Diabolepis- Nanpanaspis
450				Lochkovian	Lianhuashanian	Spirigerina supermarginalis		Gomphonchus lujingensis	Cheiracanthoides dolosus	Diabolepis- Nanpanaspis		
452	Lochkovian	Lianhuashanian	Spirigerina supermarginalis				Gomphonchus lujingensis				Cheiracanthoides dolosus	Diabolepis- Nanpanaspis
454				Lochkovian	Lianhuashanian	Spirigerina supermarginalis		Gomphonchus lujingensis	Cheiracanthoides dolosus	Diabolepis- Nanpanaspis		
456	Lochkovian	Lianhuashanian	Spirigerina supermarginalis				Gomphonchus lujingensis				Cheiracanthoides dolosus	Diabolepis- Nanpanaspis
458				Lochkovian	Lianhuashanian	Spirigerina supermarginalis		Gomphonchus lujingensis	Cheiracanthoides dolosus	Diabolepis- Nanpanaspis		
460	Lochkovian	Lianhuashanian	Spirigerina supermarginalis				Gomphonchus lujingensis				Cheiracanthoides dolosus	Diabolepis- Nanpanaspis
462				Lochkovian	Lianhuashanian	Spirigerina supermarginalis		Gomphonchus lujingensis	Cheiracanthoides dolosus	Diabolepis- Nanpanaspis		
464	Lochkovian	Lianhuashanian	Spirigerina supermarginalis				Gomphonchus lujingensis				Cheiracanthoides dolosus	Diabolepis- Nanpanaspis
466				Lochkovian	Lianhuashanian	Spirigerina supermarginalis		Gomphonchus lujingensis	Cheiracanthoides dolosus	Diabolepis- Nanpanaspis		
468	Lochkovian	Lianhuashanian	Spirigerina supermarginalis				Gomphonchus lujingensis				Cheiracanthoides dolosus	Diabolepis- Nanpanaspis
470				Lochkovian	Lianhuashanian	Spirigerina supermarginalis		Gomphonchus lujingensis	Cheiracanthoides dolosus	Diabolepis- Nanpanaspis		
472	Lochkovian	Lianhuashanian	Spirigerina supermarginalis				Gomphonchus lujingensis				Cheiracanthoides dolosus	Diabolepis- Nanpanaspis
474				Lochkovian	Lianhuashanian	Spirigerina supermarginalis		Gomphonchus lujingensis	Cheiracanthoides dolosus	Diabolepis- Nanpanaspis		
476	Lochkovian	Lianhuashanian	Spirigerina supermarginalis				Gomphonchus lujingensis				Cheiracanthoides dolosus	Diabolepis- Nanpanaspis
478				Lochkovian	Lianhuashanian	Spirigerina supermarginalis		Gomphonchus lujingensis	Cheiracanthoides dolosus	Diabolepis- Nanpanaspis		
480	Lochkovian	Lianhuashanian	Spirigerina supermarginalis				Gomphonchus lujingensis				Cheiracanthoides dolosus	Diabolepis- Nanpanaspis
482				Lochkovian	Lianhuashanian	Spirigerina supermarginalis		Gomphonchus lujingensis	Cheiracanthoides dolosus	Diabolepis- Nanpanaspis		
484	Lochkovian	Lianhuashanian	Spirigerina supermarginalis				Gomphonchus lujingensis				Cheiracanthoides dolosus	Diabolepis- Nanpanaspis
486				Lochkovian	Lianhuashanian	Spirigerina supermarginalis		Gomphonchus lujingensis	Cheiracanthoides dolosus	Diabolepis- Nanpanaspis		
488	Lochkovian	Lianhuashanian	Spirigerina supermarginalis				Gomphonchus lujingensis				Cheiracanthoides dolosus	Diabolepis- Nanpanaspis
490				Lochkovian	Lianhuashanian	Spirigerina supermarginalis		Gomphonchus lujingensis	Cheiracanthoides dolosus	Diabolepis- Nanpanaspis		
492	Lochkovian	Lianhuashanian	Spirigerina supermarginalis				Gomphonchus lujingensis				Cheiracanthoides dolosus	Diabolepis- Nanpanaspis
494				Lochkovian	Lianhuashanian	Spirigerina supermarginalis		Gomphonchus lujingensis	Cheiracanthoides dolosus	Diabolepis- Nanpanaspis		
496	Lochkovian	Lianhuashanian	Spirigerina supermarginalis				Gomphonchus lujingensis				Cheiracanthoides dolos	

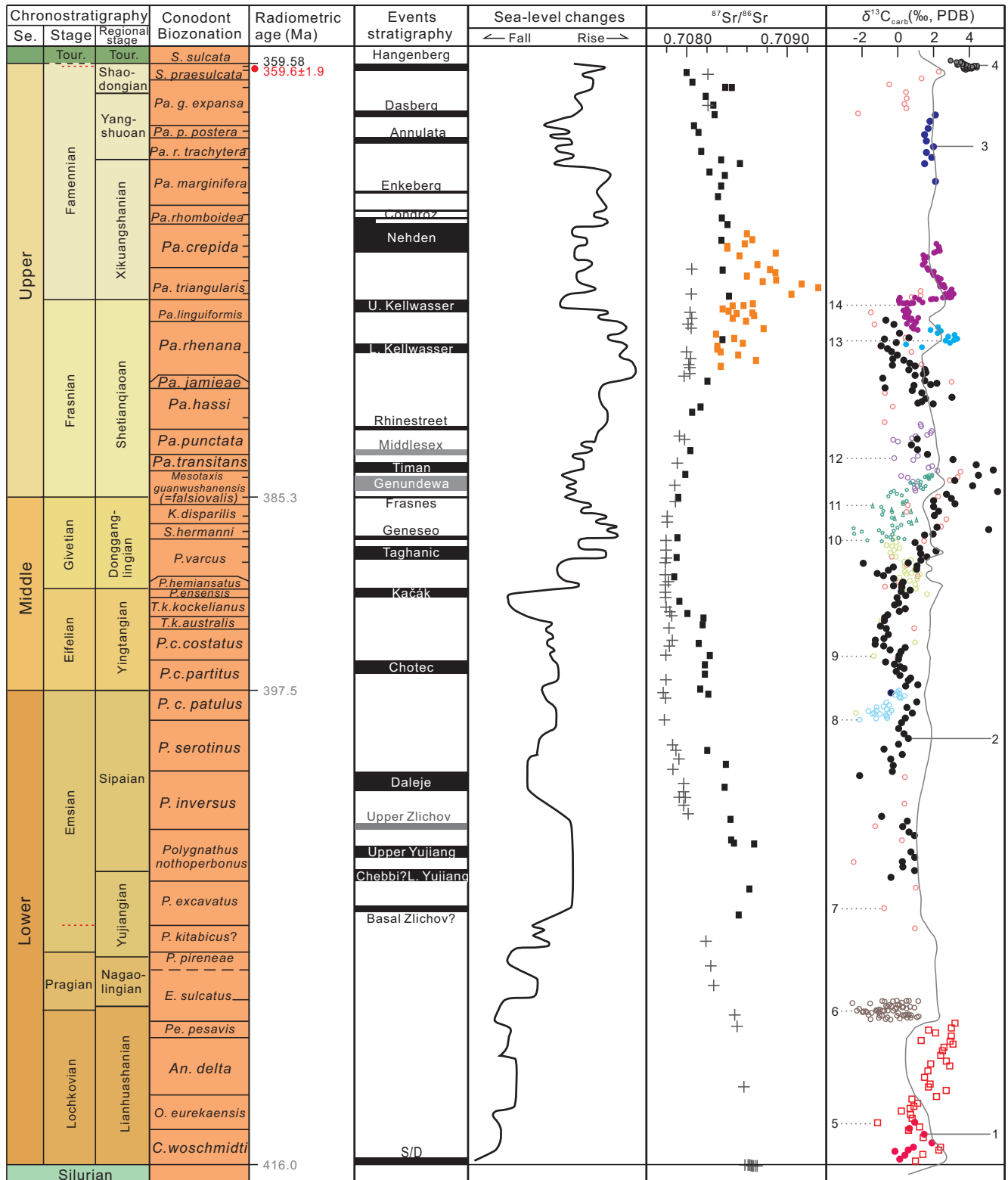


Figure 3 Generalized Devonian carbon and strontium isotope stratigraphy, event stratigraphy in China. Radiometric age is after Liu et al. (2012). Relative sea-level change curve is after Ma et al. (2009). ⁸⁷Sr/⁸⁶Sr values shown as cross are from GTS 2012, and ⁸⁷Sr/⁸⁶Sr values from South China as black and orange solid rectangle are after Huang (1997) and Chen et al. (2015), respectively. Carbon isotopic records are from: 1. Dahaiba, Baoshan; 2. Longmenshan, Mianyang; 3. Tieshan, Guilin; 4. Qilinzhai, Dushan (Qie et al., 2015); 5. Three Rivers Region (Ma et al., 2017a); 6. Dashatian, Nanning; 7. Longmenshan, Mianyang (Cui et al., 1993); 8. Maanshan, Xiangzhou (Wang et al., 2014); 9. Liuqing, Hengxian (Liu and Bai, 2009); 10. Maanshan, Xiangzhou (Wang and Bai, 2002); 11. Baqi, Xiangzhou (Wang and Bai, 2002); 12. Longmen, Guilin (Ma et al., 2008); 13, 14. Fuhe, Guilin (Xu et al., 2012; Chen et al., 2013). Locfit curve (light grey line) of carbon isotopic records from Laurussia is after Buggisch and Joachimski (2006).

the basal Devonian boundary, are marked by the FAD of certain conodont species (Table 1). The international conodont biostratigraphic sequence, consisting of 68 biozones (hundreds of thousands of years to millions of years in duration), is the basis for division and correlation of marine sediments, and provides a high-resolution timescale framework for the Devonian System (Figure 1). Researches on conodont fauna from deep-water facies by Wang (1989), Ji and Ziegler (1993), and Bai et al. (1994) have elaborated the conodont biostratigraphic sequences of Devonian in South China, and enabled the international correlation. By summarizing the taxonomy and biostratigraphy of conodonts in China, Wang (2018) confirmed 58 Devonian conodont zones in pelagic facies, among which the biozones of Emsian to Famennian can be precisely correlated to the standard international conodont zones (Figure 1).

The basal Lochkovian boundary, i.e., the basal Devonian boundary, is marked by the FAD of graptolite *U. uniformis* (Přibyl, 1940) (Table 1). When the GSSP was first established, trilobite *Walburgella rugulosa rugose* and conodont *Caudicriodus woschmidti* were used as ancillary markers in determining the boundary. In China, *C. woschmidti* has been reported in the Xiaputonggou Formation of northern Sichuan, the Rongshu Formation of western Sichuan, the Shanjiang Formation of western Yunnan, and the Alugong Formation of Inner Mongolia, that have been considered as the lowermost Devonian in China (Wang, 1981; Wang, 2006; Wang et al., 2009). However, Carls et al. (2007) suggested that many conodont species similar to *C. woschmidti* started to appear in the earliest Devonian during the radiation of the primitive icriodontids, and the first occurrence of the standard *C. woschmidti* was in fact above that of *C. post-woschmidti*, much higher than the Silurian-Devonian Boundary. Hence, whether the “*C. woschmidti*” in China can be the index of basal Devonian boundary and also the validity of the *C. woschmidti* Zone need further investigations.

The conodont zones of the Lochkovian and Pragian stages (Lower Devonian), are established mainly based on the evolutionary sequences of icriodontids (*Caudicriodus*, ‘*Icriodus*’, ‘*Pelekysgnathus*’, *Latericriodus*, and transitional types), icriodellids (*Pedavis*), spathognathodontids (*Ancyrodelloides*, *Lanea* and *Masaraella*), and eognathodontids (*Eognathodus*, *Gondwania* and *Pseudogondwania*). During the Lochkovian and Pragian, endemic conodont taxa were well developed due to the low sea level and biogeographic provincialism, and thus standard global conodont zonation is unachievable (Murphy, 2005; Slavik et al., 2012). Due to the lack of systematic researches on the type sections, the Lochkovian conodont zones in China are only preliminarily established based on sporadic records of index taxa in Inner Mongolia, Xinjiang, western Yunnan, Sichuan, and Tibet, and need further improvement (Bai et al., 1982; Wang and Ziegler, 1983; Xia, 1997; Wang, 2006; Wang et al., 2009)

(Figure 1).

The FAD of conodont *Eognathodus sulcatus* marks the basal Pragian boundary (Chlupáč and Oliver, 1989), but this viewpoint is controversial owing to taxonomic uncertainty and the different occurrence levels around the world. The primitive elements of *Eognathodus* from the stratotype section was recently reclassified as *E. irregularis*, with its first occurrence below the current GSSP horizon, while the standard *E. sulcatus* appear in the middle Pragian. Thus, it should not be served as the index species for the basal Pragian boundary (Becker et al., 2012). The Pragian conodont zonations in China have not been well studied, with merely sporadic records and incomplete sequences. In a recent work, Wang et al. (2016) identified *E. irregularis*, *E. nagaoilingensis*, *E. sulcatus* and *Masaraella pandora* from the Nahkaoling Formation of the Dashatian section, Nanning, Guangxi, assigned the horizons to lower Pragian, and correlated it to the *E. irregularis-Gondwania profunda* Zone in North America and the *E. sulcatus* Zone in Europe. Besides, the Nahkaoling Formation and lower Shizhou Member of the Yukiang Formation in the Liujing section, Hengxian, Guangxi, were reported to yield *Polygnathus pireneae*, *P. sokolovi*, *E. sulcatus*, *E. nagaoilingensis* and *E. kuangi*, and could be correlated to the *E. kindlei* to *P. pireneae* Zone in Europe (Lu et al., 2016).

The GSSP of the Emsian Stage is under revision in terms of the low appearance horizon of the index taxon *P. kitabicus* at the Zinzilban stratotype section, Uzbekistan, which cut nearly 2/3 of the traditional underlying Pragian Stage (Carls et al., 2008). The SDS meeting voted for a decision to raise the basal Emsian boundary to a level close to the entry of *P. excavatus* Carls & Gandl, 1969 in order to correlate more closely with the classical Emsian in Rheine region of Germany. One potential choice for the new GSSP is the entry of *P. excavatus* ssp. 114 (Carls et al., 2008). In South China, researches on the basal Emsian conodont sequences in Tiandeng, Nandan, and Hengxian, Guangxi suggest that the uppermost Nahkaoling Formation is correlative to the Pragian *P. pireneae* Zone, and that both *P. e. excavatus* and *P. e. ssp. 114* exist in the Yilan Formation and the middle Shizhou Member of the Yukiang Formation, but precise horizons of the lowermost part of the *P. excavatus* Zone and the underlying *P. kitabicus* Zone remain uncertain (Lu et al., 2016; Guo, 2017).

During the Emsian to Famennian, distribution and evolution of conodonts tended to be cosmopolitan as a result of the global sea level rise, which enables a precise conodont biostratigraphic correlation in pelagic facies around the world. *Polygnathus* and *Icriodus* are two representative conodonts genera from the Emsian to the middle Givetian, and the former is the key taxon in division of conodont zones. The evolutionary lineage of polygnathids, *Polygnathus pireneae*→*P. kitabicus*→*P. excavatus*→*P. perbonus*→*P.*

nothoperbonus→*P. inversus* (Yolkin et al., 1994), was the basis for biostratigraphic frame of the Emsian Stage. The occurrences of their descendants, *P. c. partitus* and *P. hemiansatus*, represent the base of the Eifelian and Givetian, respectively (Table 1). Many taxa with rapid evolution and short range (e.g., *Ancyrognathus*, *Ancyrodella*, *Klapperina*, *Mesotaxis*, and *Schmidtognathus*) occurred during the late Givetian to the Frasnian, which is consistent with severe climate fluctuations and multiple biological and environmental events, and the basal Frasnian was marked by early form of *Ancyrodella rotundiloba* (Table 1). Many above mentioned representative taxa of the Middle Devonian became extinct during the F-F event and gave way to the prosperity of palmatolepids in the early-middle Famennian. Later after the Dasberg Event in the Late Famennian, palmatolepids declined and finally died out around the DCB. Meanwhile, conodont taxa, such as *Pseudopolygnathus*, *Siphonodella*, *Bispathodus* and *Protognathodus*, occurred and replaced the significance of palmatolepids in biostratigraphic division. In South China, the Emsian to Givetian conodont biozones were established mainly based on the Liujing section of Hengxian, the Dale section of Xiangzhou and the Sihongshan section of Debao, Guangxi Province (Bai et al., 1982, 1994; Wang, 1989; Lu et al., 2016), while the Frasnian and Famennian zones on the Luofu section of Nandan and the Lali section of Yishan, Guangxi Province (Zhong et al., 1992; Ji and Ziegler, 1993).

The Nanbiancun section in Guilin, Guangxi is one of the auxiliary stratotype sections for the global Devonian-Carboniferous boundary, and the GSSP is located at the bottom of Bed 89 in the La Serre section, France and marked by the FAD of conodont *S. sulcata* in the *S. praesulcata*-*S. sulcata* evolutionary lineage (Table 1). Recent studies indicated that *S. sulcata* actually shows its first occurrence at the bottom of Bed 84 in the La Serre Section, near a lithological interface resulted from an event deposit (Kaiser, 2005). Besides, the *S. praesulcata*-*S. sulcata* evolutionary lineage is far from clarified for the existences of several morphotypes of *S. praesulcata* (Kaiser and Corradini, 2011). The DCB working group of ICS decided to lower the boundary to one level of the following candidates: the FAD of conodont *Pr. kockeli*, the beginning of biodiversification of the Carboniferous-type organisms, the end of the Hangenberg mass extinction, or the end of the latest Devonian regression (Spalletta et al., 2017). Numerous DCB sections recording various sedimentary facies and abundant fossils are well exposed in China. Based on the integrated studies of the conodont biostratigraphy, carbon isotope stratigraphy and event stratigraphy, the Hangenberg Event and the DCB by the present definition have been precisely located in both deep-water and shallow-water facies in South China (Qie et al., 2015, 2016). The *Protognathodus* fauna has also been reported from the Nanbiancun section of Guilin, Guangxi Province, as well as

the Muhua and Daposhang sections, Guizhou Province (Hou et al., 1985; Yu, 1988; Ji et al., 1989), but further researches are still needed since the complete evolutionary sequence of *Pr. meischneri*→*Pr. collinsoni*→*Pr. kockeli* has not been precisely identified yet in South China.

3.1.2 Graptolite

Early Devonian graptolites have been reported in Qinzhou, Yulin, Guangxi Province, western Yunnan Province, as well as Tibet, with stratigraphic range up to the lower Emsian. The graptolite biozones established by Mu et al. (1988) and Wang (1988) have been widely applied in stratigraphic division and correlation. Chen et al. (2015) carried out a detailed research about the graptolites in the Qinzhou Formation of Qinzhou-Yulin area, recognized 3 genera and 14 species, and identified the following 4 biozones: the *U. uniformis* Zone, the *U. praehercynicus* Zone, the *Neomonograptus falcarius* Zone, and the *U. yukonensis* Zone in ascending order, which could be correlated to the biozones in Prague area. The graptolite *U. uniformis* has also been found in Shidian and Ximeng, western Yunnan, and the base of the *U. uniformis* Zone defines the Silurian-Devonian Boundary in China. The *N. himalayensis* Zone, established by Mu and Ni (1975), was reported in the lower part of the Liangquan Formation in Nielamu area, southern Tibet, and the accompanying tentaculite *N. acuaria* indicates a horizon of lower-middle Pragian (Figure 1).

3.1.3 Ostracod

Biostratigraphic sequences of Devonian pelagic ostracods, especially the entomozoacean, have been completed in South China, which comprise 19 zones and 4 subzones, and played a key role in stratigraphic division and correlation of deep-water sediments devoid of conodonts or ammonoids (Wang, 2009). Seven entomozoacean range-zones of lower and middle Devonian, namely the *Monosulcoentomozoe beijuntangensis* Zone, the *Trisulcoentomozoe trisulcata* Zone, the *Bisulcoentomozoe tuberculata* Zone, the *Richteria longisulcata* Zone, the *R. nanyiensis* Zone, the *Bertillonella praeerecta* Zone and the *B. suberecta* Zone from the bottom up, were established in Zhangmu of Yulin and Luofu of Nandan, Guangxi (Wang, 1983, 1986). In upper Devonian of South China, 12 ostracod zones and 4 subzones have been identified, and can be precisely correlated to those of Europe (e.g., Rheine area of Germany, Groos-Uffner et al., 2000). The entomozoacean zones of the upper Frasnian serve as an even higher-resolution standard than conodont zones in stratigraphic division (Wang, 2009; Song and Gong, 2015) (Figure 1). Besides, Wang and Peng (2005) established 11 leperditicoid assemblages in the shallow-water facies of South China and adjacent areas according to stratigraphic ranges and the ratio of height of the V-shaped muscle scar to that of the adductor muscle scar (th/ah) in the Sinoleperdi-

tiinae ostracods. The assemblage biozones enable stratigraphic division and correlation in South China and South-east Asia.

3.1.4 Brachiopod

The Devonian brachiopod assemblages are extensively applied in stratigraphic division and correlation of shallow-water successions in South China. Many unit-stratotypes of the Chinese regional stages, such as the Nagaolingian, Yujiangian, Yingtangian, Shetianqiaoan, and Xikuangshanian, are defined by occurrences of certain wide-spread brachiopod fauna (Table 1). During the Lochkovian time, near-shore clastic sediments widely developed in most area of South China as a result of the Kwangshian Orogeny, and the brachiopod *Spirigerina supramarginalis* fauna, represented by *Grayina*, *Vagrana*, *Macrophura*, *Isothis*, *Reticulatripa*, etc., was restricted to the deep-water environment in Qinzhou, Guangxi Province (Hou et al., 1988). During the Pragian to Famennian, brachiopod flourished in South China, and the following 11 assemblage/acme zones have been identified from bottom up in shallow-water facies (Hou, 1981; Tan, 1987; Ma et al., 2009; Ma and Zong, 2010; Hou et al., 2017): *Orientospirifer nakaolingensis* Zone, *Rostrospirifer tonkinensis-Dicoelostrophia* Zone, *Howellella fecunda-Reticulariopsis ertangensis* Zone, *Trigonospirifer-Otospirifer-Euryspirifer* Zone, *Athyrisina-Yingtangella-Xenospirifer* Zone, *Stringocephalus* Zone, “*Leiorhynchus*” Zone, *Cyrtospirifer* Zone, *Yunnanella-Sinospirifer* Zone, *Nayunnella-Huanospirifer* Zone, and *Yanguania dushanensis-Trifidorostellum longhuiense-Plicochonetes ornatus* Zone (Figure 2). In addition to the above-mentioned shallow-water faunas, other types of brachiopod fauna have also been reported in South China as a result of the differentiation of sedimentary facies and biofacies during the early Emsian to the Famennian. A monotonous brachiopod fauna dominated by the small-sized and double-spined athyrid, *Sinathyris*, was reported in the deep-water sediments of the Upper Yilan Formation in Nandan, Guangxi (Guo et al., 2015), which was contemporary with the *Howellella fecunda-Reticulariopsis ertangensis* assemblage zone of the shallow-water facies. Later in the Nandan area, the *Costanoplia-Plectodonta* fauna represented by thin-shelled and small-sized brachiopods appeared in the Tangxiang Formation (Xu, 1977, 1979), corresponding to the *Trigonospirifer-Otospirifer-Euryspirifer* assemblage zone of the shallow-water facies, and meanwhile in the platform margin facies, the existence of *Zdimir* assemblage zone was widely reported (Wu and Yan, 1980; Bureau of Geology and Mineral Resources of Guangxi, 1985; Kuang et al., 1989). During the middle Devonian, transitional facies developed in the Liujing area, Guangxi Province. The brachiopod fauna characterized by *Vallomyonia (Yujiangella) sinensis*, *Pentamerella nanningensis*, and *Cyrtinoides guangxiensis* (= *Echiinocoelia*

guangxiensis Sun), and the *Stringocephalus-Changtangella* fauna were reported in the uppermost Eifelian and the lowermost Givetian, respectively (Sun, 1992; Bai et al., 1994; Xian, 1998; Baliński and Sun, 2016). A monotonous brachiopod fauna dominated by the rhychonellid *Dzieduszyckia* existed in the off-shore carbonate platform facies and the intra-platform basinal facies of Guangxi and Guizhou during the early Famennian (Nie et al., 2016). In the regional Yangshuoan (roughly corresponding to the conodont *Pa. r. trachytera* to *Pa. p. postera* zones), no brachiopod assemblage zone has been identified yet in South China due to rare existence of brachiopods (Figure 2).

3.1.5 Coral

Rugose and tabulate corals are important fossil groups in Devonian marine strata. They were abundant, diverse, and evolved rapidly in shallow marine environment, often forming complex reef systems together with stromatoporoids and algae (Liao, 2006). During the Devonian time, corals have experienced five major turnover events (Liao, 2006, 2015): (1) the occurrences of earliest representatives of Pragian rugose corals, such as *Chalcidophyllum* and *Eoglossophyllum*, indicating the disappearance of Silurian-type corals and the appearance of Devonian-type corals (Wang et al., 1974); (2) in the middle Eifelian, favositids (such as *Favosites*, *Squameofavosites* and *Dictyofavosites*), heliolitids (such as *Heliolites*), and some important coral species became extinct; (3) the late Givetian event caused the extinction of cystimorph corals such as *Mesophyllum*, *Cystiphyllodes* and *Calceola*; (4) the F-F extinction event led to the demise of most Devonian-type corals, leaving just a few species such as *Smithiphyllum* in sporadic localities in South China during the early to middle Famennian; (5) in late Famennian, Carboniferous-type corals started to appear, indicated by abundant endemic elements in South China, such as *Ceriphyllum* and *Cystophrentis*.

By summarizing taxonomy and evolution of Devonian rugose corals from South China, Liao and Ruan (2003) proposed 14 rugose coral zones for regional stratigraphic subdivision and correlation (Figure 2). In contrast, coral faunas from other regions in China (such as Junggar and Tibet) have not been well studied, and no complete coral biostratigraphic sequence was established. In South China, the lowest Devonian rugose coral zone is the *Chalcidophyllum-Eoglossophyllum* zone of Pragian; the Emsian Stage contains five zones, listed here in ascending order: *Xystriphylloides-Heterophaulactis*, *Siphonophrentis-Stereolasma*, *Lyrielasma-Xiangzhouphyllum*, *Trapezophyllum*, and *Psydracophyllum-Leptoinophyllum* zones; the Eifelian Stage corresponds to the *Utaratuia-Brevisseptophyllum* zone; the Givetian Stage includes *Dendrostella-Columnaria* and *Endophyllum-Sunophyllum* zones; the Frasnian Stage comprises *Sinodisphyllum* and *Peneckiella-Pseudozaphrentis*

zones; the Famennian Stage is composed of *Smithiophyllum*, *Ceriphyllum*, and *Cystophrentis* zones (Figure 2).

3.1.6 Microspores

Devonian microspores evolved quickly, characterized by high abundance, and are the most useful fossils to make correlation between marine and terrestrial sediments. Nevertheless, it is hard to establish high-resolution standard palynostratigraphic sequence for international and regional correlation due to commonly incomplete terrestrial and non-marine successions, flora provincialism and vegetation zoning within certain areas. Ouyang et al. (2017) studied and reviewed a total of 50 Devonian palynological assemblages from South China, Junggar, Tarim, Qinling and Tibet, and managed to make a preliminary correlation using integrated biostratigraphic framework. The palynostratigraphic sequence in Figure 2 was mainly based on the microspore assemblages from Qujing, Yunnan (NC, GC, VL and RCA), Liujing, Guangxi (LP, RAS, and VMC), Dushan, Guizhou (TA and DG), Changyang, Hubei (CD), Xikuangshan, Jieliang and Xinshao, Hunan (LH-LN) (Gao, 1990; Ouyang et al., 2017). It should be noted that the palynological assemblages of uppermost Famennian enable high resolution stratigraphy correlation, among which, the *Retispora lepidophyta-Knoxisporites literatus* (LL), *R. lepidophyta-Hymenozonotriletes explanatus* (LE), and *R. lepidophyta-Verrucosisporites nitidus* (LN) can be recognized at a global scale (Becker et al., 2012).

3.1.7 Plants

In recent years, Chinese paleobotanists made important progresses regarding the systematic taxonomy and evolution biology (Wang and Xu, 2005; Xue, 2009). Some plant groups, such as traditional *Protolpidodendron* has been revised and correlated globally (Xu and Wang, 2008). New advances in Devonian flora (Hao and Xue, 2013; Xu et al., 2015), plant palaeogeography (Xu et al., 2014), and geochronology (Zheng et al., 2016) provide important basis for the further study on terrestrial stratigraphy in China.

As for paleobiogeography of the Devonian floras of China, two realms, i.e., the North and South Realms, could be differentiated based on divergent plant assemblages (Cai and Wang, 1995). Notably, the South Realm has been extensively studied and several Devonian floras have been recognized, including the Pragian Posongchong Flora (Hao and Xue, 2013), the late Pragian to earliest Emsian Xujiachong Flora (Wang et al., 2002), the late Middle Devonian Xichong Flora (Wang et al., 2007) and the Late Devonian Wutong Flora (Wang et al., 2006). In China, Eifelian horizons with plant fossils are quite limited, and till now, were only found in the Hujiersite Formation of Tacheng, Xinjiang, yielding *Serrulacaulis spineus* and *Planatophyton hujiersitense* (Xu et al., 2011; Gerrienne et al., 2014). Based on the recent progresses,

we establish a new plant biostratigraphic sequence at a stage level, consisting of the Lochkovian *Zosterophyllum-Xitunia* assemblage zone, the Pragian *Zosterophyllum-Yunia* assemblage zone, the Emsian *Psilophyton-Hsia* assemblage zone, the Eifelian *Serrulacaulis* assemblage zone, the Givetian *Minarodendron-Leclercqia* assemblage zone, the Frasnian *Archaeopteris-Leptophleoum* assemblage zone, and the Famennian *Sublepidodendron-Shougangia-Hamatophyton* assemblage zone (Figure 2).

3.2 Carbon isotopic stratigraphy

Devonian $\delta^{13}\text{C}_{\text{carb}}$ curves from Euramerica have been established by Buggisch and Joachimski (2006) and Saltzman and Thomas (2012), but the isotopic patterns in different sections and regions can be quite different. Before the use of $\delta^{13}\text{C}_{\text{carb}}$ records to facilitate high resolution correlation, it is necessary to conduct sedimentary facies and diagenesis analyses and compare numerous isotopic records on a global scale, in order to learn the global versus local contribution in a $\delta^{13}\text{C}$ record.

Around the Silurian-Devonian boundary in China, carbon isotope ratios show a major positive excursion with an amplitude of 1.4‰ and 2‰ in the Three Rivers Region and western Yunnan, respectively (Figure 3). The carbon isotope excursion was previously reported from Prague syncline, Carnic Alps and North America, with peak values around 3.8‰. In Nevada, $\delta^{13}\text{C}$ excursion reaches 5.8‰, and this shift represents the largest Devonian $\delta^{13}\text{C}$ event (Buggisch and Joachimski, 2006; Saltzman and Thomas, 2012; Husson et al., 2016). In China, $\delta^{13}\text{C}$ values abruptly decrease to values around 0.6‰ during the middle Lochkovian, and are followed by a gradual increase with maximum values around 3.2‰ in the top Lochkovian (Figure 3). The $\delta^{13}\text{C}$ curve in the Three Rivers Region is similar to North America, showing the second increase in the middle Lochkovian, while in Prague, the second positive shift of $\delta^{13}\text{C}$ occurred in the top Lochkovian (Buggisch and Joachimski, 2006) (Figure 3).

Few Pragian carbon isotopic records have been reported in China, and our recent study fills this gap, and shows that $\delta^{13}\text{C}$ values in the *E. sulcatus* zone at Dashatian, Nanning, Guangxi are between -2.5‰ and 1‰, characterized by major fluctuations (Figure 3). Meanwhile, the trace element and sedimentary facies analyses further suggest that the $\delta^{13}\text{C}$ records in the studied area are intensely influenced by the meteoric diagenesis and re-mineralization of organic matter, and cannot be used for stratigraphic correlation over large distances.

Previous researches on the Emsian $\delta^{13}\text{C}_{\text{carb}}$ records focused on the Longmenshan section of Mianyang, Sichuan Province, the Bahe section of Tiandeng and the Maanshan section of Xiangzhou, Guangxi Province. However, due to the low-resolution sampling and poor biostratigraphic control,

previous $\delta^{13}\text{C}$ records cannot be correlated with their counterparts in Europe (Figure 3). New carbon isotope data are derived from the Longmengshan section of Mianyang, indicating that the Emsian $\delta^{13}\text{C}_{\text{carb}}$ values in South China are between -1‰ and 0.9‰ , around 0, and generally lower than contemporary $\delta^{13}\text{C}$ values in Europe (Buggisch and Joachimski, 2006) (Figure 3). Emsian $\delta^{13}\text{C}_{\text{carb}}$ records in South China, Europe and North America stay stable with only minor fluctuations, and a slow trend towards higher values is observed in upper Emsian (Figure 3).

At Longmenshan, $\delta^{13}\text{C}$ values decrease from around 1.2‰ to -1.3‰ in the lower Eifelian and are followed by a gentle increase to values around 0.7‰ near the base of the Givetian with an amplitude of 2‰ . $\delta^{13}\text{C}_{\text{carb}}$ values of brachiopods from Germany and Morocco record a major positive excursion in the middle Eifelian and increase from around 0.5‰ to 2.6‰ . Then, $\delta^{13}\text{C}_{\text{carb}}$ values decline to around 1.1‰ , and across the Eifelian-Givetian boundary, show an abrupt increase to maximum values around 3‰ . During the Eifelian, $\delta^{13}\text{C}$ patterns recovered from different regions and sample materials are quite different, and need to be further confirmed (Buggisch and Joachimski, 2006; van Geldern et al., 2006). But in all studied sections, a significant positive shift of $\delta^{13}\text{C}$ with a similar amplitude has been recognized near the Eifelian-Givetian boundary, indicating a possible global carbon isotope event.

Many carbon isotope studies on the Givetian in South China have been conducted, and mainly focused on the Dale and Maanshan sections of Xiangzhou, the Liujing section of Hengxiang, Guangxi, and the Longmenshan section of Mianyang, Sichuan Province (Cui et al., 1993; Bai et al., 1994; Wang and Bai, 2002). $\delta^{13}\text{C}$ values are generally between -2‰ and 2.5‰ , and the evolution patterns cannot be well correlated due to the poor biostratigraphic control and the different base-line values in the studied sections. Our new data indicate that $\delta^{13}\text{C}$ values show significant variations in Givetian at Longmenshan and a positive excursion is evident in the middle Givetian, with an amplitude of $>3.5\text{‰}$ (Figure 3). This isotopic shift can be recognized in Europe, and may correlate with global sea-level rise and the Givetian Taghanic event (Buggisch and Joachimski, 2006; Becker et al., 2012).

Around the Givetian-Frasnian boundary, carbon isotope ratios show a major positive shift, with an amplitude of 2.5‰ and 3‰ in the Maanshan and Longmenshan sections, respectively (Figure 3). The excursion reaches 5.6‰ in the Longmenshan section, which represents the peak $\delta^{13}\text{C}$ value of Devonian marine carbonates in China. In France, Italy, Germany and Australia, it is also recognized in the middle *M. falsovalis* zone of basal Frasnian, with an amplitude of about 2‰ and peak values $<4.4\text{‰}$ (Buggisch and Joachimski, 2006). In the lower Frasnian, $\delta^{13}\text{C}$ values show significant fluctuations, but no uniform pattern has been established at a global scale; in the upper Frasnian, consistent with the lower

and upper Kellwasser events, $\delta^{13}\text{C}$ values show two major positive shifts, respectively. The shift amplitudes ($\sim 3\text{‰}$) and peak values ($\sim 3.5\text{‰}$) of these two excursions can be observed around the world, indicating global carbon isotopic events during this critical time interval (Joachimski et al., 2002; Stephens and Sumner, 2003; Chen et al., 2005; Xu et al., 2012; Chang et al., 2017) (Figure 3).

A large, positive carbon isotope excursion across the Frasnian-Famennian boundary was reported in the Fuhe and Baisha sections, South China, and reaches the maximum value near the base of the middle *Pa. triangularis* zone. Following the peak values, $\delta^{13}\text{C}$ shows a gradual decreasing trend to around 1.1‰ , which is interrupted by a minor positive shift in the lower to middle *Pa. crepida* zone (Chen et al., 2013; Chang et al., 2017). In South China, no carbon isotopic record has been reported in the upper *Pa. crepida* zone and lower *Pa. marginifera* zone, while in Europe, $\delta^{13}\text{C}$ values fluctuate between 1‰ and 2‰ (Buggisch and Joachimski, 2006). At the Tieshan section, $\delta^{13}\text{C}$ values remain stable (around 2‰) in the middle *Pa. marginifera* zone to the lower *Pa. g. expansa* zone, and is consistent with the records in Europe (Figure 3). In uppermost Devonian of South China, our recent $\delta^{13}\text{C}$ data document a negative excursion within the middle *S. praesulcata* zone (i.e., the Hangenberg mass extinction interval) and a major positive $\delta^{13}\text{C}$ shift in the upper *S. praesulcata* zone (HICE) (Qie et al., 2015). However, local carbon cycling processes played an important role, and the peak $\delta^{13}\text{C}$ values and the magnitude of the HICE differ markedly in different sedimentary settings. In the shallow-water near-shore platform, $\delta^{13}\text{C}$ values show a prominent positive shift increasing by $>4\text{‰}$ to 4.5‰ in the Qilinzhai section, while in the deep-water basin, $\delta^{13}\text{C}$ values in the Gedongguan section fluctuate around 2‰ and display merely a minor shift with an amplitude of about 1‰ . The temporal and spatial compositions of carbon isotopic records in South China can be correlated with Belgian-France Basin and Carnic Alps, and have important global significance during the Devonian-Carboniferous transition (Qie et al., 2015).

3.3 Strontium isotope stratigraphy

Since the residence time of Sr in the ocean ($\sim 10^6\text{a}$) is far longer than the ocean mixing time ($\sim 10^3\text{a}$), the world's oceans are considered homogeneous with respect to seawater $^{87}\text{Sr}/^{86}\text{Sr}$, which has long been used as a tool for precise stratigraphic correlation and dating (McArthur et al., 2012). Huang (1997) reported a $^{87}\text{Sr}/^{86}\text{Sr}$ record of the Emsian to Famennian using marine carbonates from the Longmenshan section, Sichuan Province. $^{87}\text{Sr}/^{86}\text{Sr}$ values are $0.70788\text{--}0.70868$, and its long-term trend agrees with a published mean LOWESS fitted line (Figure 3). After a gradual decline

from early Devonian, $^{87}\text{Sr}/^{86}\text{Sr}$ ratios reach nadir values and stay stable in middle Devonian, then start to increase in Frasnian and define a plateau throughout the Famennian. However, the existing standard Devonian seawater $^{87}\text{Sr}/^{86}\text{Sr}$ record remains poorly resolved in the Lochkovian to lower Emsian, and no data have been reported from the upper Famennian, leading to stratigraphic uncertainties and poor correlation using strontium isotopic records from South China. Notably, the Emsian to upper Eifelian and upper Frasnian $^{87}\text{Sr}/^{86}\text{Sr}$ values at Longmenshan are scattered and much higher than the mean LOWESS fitted line (Figure 3), reflecting possible influences of regional geological events (Huang et al., 2002). Chen et al. (2005) conducted high-resolution strontium isotope analyses of marine carbonates in the Frasnian-Famennian boundary intervals at the Fuhe and Baisha section of Guilin, Guangxi. $^{87}\text{Sr}/^{86}\text{Sr}$ values fluctuate between 0.7082 and 0.7094, and show two major positive shifts in the Lower and Upper Kellwasser horizons (Figure 3), respectively, which are also consistent with two major positive excursions of $\delta^{13}\text{C}_{\text{carb}}$ and $\delta^{13}\text{C}_{\text{org}}$ pairs. Chen et al. (2005) suggest that the climatic perturbations, triggered initially by enhanced volcanic activity and subsequent increased riverine nutrient fluxes and primary productivity, in together with marine anoxia lead to the stepwise mass extinction during the Frasnian-Famennian transition. Nevertheless, $^{87}\text{Sr}/^{86}\text{Sr}$ values in the Fuhe and Baisha sections varied considerably, and are much higher than the data from the mean LOWESS fitted line (Figure 3), whether they reflect possible diagenetic alteration, regional geological events or restricted water mass need further evaluation.

3.4 Devonian event stratigraphy

As many as 25 events, characterized by sea-level rise and fall, ocean anoxic/hypoxic events, and/or biological extinctions/turnovers, took place during the Devonian (Becker et al., 2012). All these events were closely related to the climate changes resulted from the Milankovitch cycles, featured by ‘isochroneity’ and ‘instantaneity’. For example, the main episode of the F-F mass extinction lasted for 0.2–0.4 Ma (the Upper Kellwasser horizon; De Vleeschouwer et al., 2013; Huang and Gong, 2016), while duration of the main episode of the end-Devonian Hangenberg extinction was only 0.05–0.1 Ma (middle *S. praesulcata* Zone, Myrow et al., 2013), and thus identification of these events in stratigraphic sequences enables a higher-resolution correlation of Devonian. A brief introduction of the Devonian events in South China has been made by Ma et al. (2014), and here in the following section, we will discuss the major biological and environmental events in detail.

3.4.1 The Silurian-Devonian Boundary (S/D) Event

The S/D event represented the biotic recovery after the

Transgrediensis extinction, and was characterized by simultaneous appearance of the Devonian-type organisms at a global scale, such as the graptolite *U. uniformis*, *U. subhercynicus*, *Neomonograptus aequabilis* and conodont *Caudicriodus*, and by a significant positive shift of carbon isotope (Buggisch and Joachimski, 2006; Manda and Fryda, 2010). In China, this positive shift of carbon isotope was also identified around the S/D boundary in the Putongou and Yanglugou sections of western Qinling area, the Xishancun section of Qujing, Yunnan Province, and the Changwantang section of Yunlin, Guangxi (Zhao et al., 2011, 2015). These carbon isotope stratigraphic works, together with researches on conodont, microvertebrate and graptolite biostratigraphy, help to confirm the precise horizon of the S/D boundary and event in China.

3.4.2 The basal Zlichov, Chebbi, and Yujiang events in early Emsian

Clastic sedimentary facies were widely spread in South China before the Emsian Stage, and massive carbonate sediments did not begin to develop until the conodont *P. excavatus* Zone. In addition, the horizon of the basal carbonate rocks in northern area is relatively higher than the southern area, which indicates a transgressive overlapping in South China during the Early Devonian. The occurrences of conodont *P. e. ssp. 114* in the upper Yilan Formation at the Mode section of Nandan and in the limestone above the Yujiang and Huangjingshan formational boundary at the Poyuan section of Tiandeng (Guo, 2017) suggest that the rapid transgression took place in the upper *P. excavatus* Zone of Emsian and can be correlated to the Basal Zlichov Event in Europe and Africa (Garcia-Alcalde, 1997; Becker and Aboussalam, 2011).

The term ‘Chebbi Event’ derived from the *Metabactrites-Erbenoceras* shale near Ouidane Chebbi of Morocco, and it occurred in the uppermost *P. excavatus* Zone (correlating to the upper *P. gronbergi* Zone in GTS2012). This event was characterized by the first radiation of ammonoids in the world, representing one of the significant events in the evolutionary history of planktons (Becker and Aboussalam, 2011). The first occurrence of ammonoids in China, including *Anetoceras*, *Erbenoceras* and *Teicherticeras*, was recorded in the tentaculitid *N. praecursor* Zone of Luofu, Nandan, Guangxi (Zhong et al., 1992; Liao and Ruan, 2003), which was very close to horizon of the Chebbi Event.

The Yujiang event was formally proposed by Yu et al. (2018), intending to represent the paleobiological and paleoenvironmental changes in South China during the early Emsian. The first episode of the Yujiang Event, corresponding to a rapid transgression event, occurred in the lowermost part of the *P. nothoperbonus* Zone, and is characterized by lithological changes, extinction of the biotreme-constructor *Xystriphylloides*, disappearance of coral

biostromes, as well as compositional change of the *Rostrospirifer tonkinensis* Fauna. The main episode of Yujiang Event was evidenced by the extinction of the *Rostrospirifer tonkinensis* Fauna in the upper part of the *P. nothoperbonus* Zone and consistent with a second transgression event. Significant differentiation of sedimentary facies occurred after the Yujiang Event in South China, and 4 sedimentary types were recognized according to lithological and biological features: the Qujing type (paralic facies), the Xiangzhou type (benthic facies), the Nandan type (pelagic facies), and the transitional facies (Hou et al., 1988) (Figure 4).

In South China, the transgression event in the lowermost *P. nothoperbonus* Zone resulted in the extinction and change-over of benthic fauna in shallow marine ecosystem, while in the deeper water region (e.g., Luofu, Nandan), ammonoids started to appear and radiate, which may reflect diverse patterns responding to the Chebbi Event in different plates and sedimentary facies.

3.4.3 The Choteč and Kačák events in Eifelian

The Choteč event represents one of the global transgression and ocean anoxia/hypoxia events that occurred in earliest middle Devonian (upper part of the *P. c. partitus* zone). It is characterized by abundant burial of organic matters and the turnover of major marine fauna groups (Walliser, 1996). In pelagic facies of South China, this event corresponds to the dark argillaceous limestones, siliceous rocks, and siliceous mudstones of the uppermost Pozheluo Formation; while in shallow-water platform facies, it is consistent with the Dale and Gupa formational boundary, marked by the occurrences of tentaculite *N. sulcata*, brachiopod *X. fongi-E. lachrymosa* assemblage and coral *Utaratuia-Brevisseptophyllum* assemblage, which indicate the beginning of the regional Yingtangian Stage (Table 1).

The Kačák event is manifested by deposition of black shale, widely distributed near the E-G boundary intervals in Europe and other regions, indicating global sea level rise, abundant burial of organic matters and marine anoxia during this time, which had a major impact on the pelagic fauna, such as conodonts, cephalopods and dacroconarid tentaculitids (Walliser, 1996; Königshof et al., 2016). In pelagic facies of South China, this event is characterized by the occurrence of tentaculite *N. otomari*; in transitional facies, it is marked by the lithological change from the dolostone of the Najiao Formation and dolomitic limestone of the lower Mintang Formation to the thin-bedded limestone containing diverse dacroconarid tentaculitids, and by simultaneous appearances of tentaculite *N. otomari* and brachiopod *Stringocephalus*; in shallow-water platform facies, a positive shift of $\delta^{13}\text{C}$ value increasing by around 2‰ is observed near the E-G boundary in the Longmenshan section, which could be a good indicator of the Kačák event (Figure 4).

3.4.4 The Taghanic and Frasnian events in Givetian

The Taghanic event (from the upper middle *P. varcus* zone to upper *Schmidtognathus hermanni* zone) is consistent with global sea-level rise, and characterized by enhanced occurrences of biotic invasion, demise of typical Givetian fauna and rapid decline of biodiversity, which represents one of the most important geological events and extinction events in Devonian (House, 2002; McGhee et al., 2013). In South China, the relative sea-level changes was influenced by local tectonic activities, i.e. intensified rifting since the middle of the lower *P. varcus* Zone, but the change pattern is basically the same with the global sea-level (Ma et al., 2009) (Figure 3). This event resulted in the replacement of the *Maenioceras* fauna by the *Pharciceras* fauna in pelagic facies; in shallow-water platform facies, it is marked by the demise of brachiopod *Stringocephalus* and the disappearance of most species of the *Endophyllum-Sunophyllum* assemblage; deeper water sequences started to occur in the transitional facies (e.g., the Gubi Formation at Liujing) and shallow-water platform facies (e.g., the Baqi Formation in Xiangzhou) (Figure 4).

The Frasnian event is recorded around the Givetian-Frasnian boundary, and represented by the sea-level transgression and biotic turnover in the Euramerican sections (House, 2002). In contrast, a major sea-level fall occurred in South China, indicated by the missing of lower Frasnian in central Hunan and northern Guangxi and the strata yielding middle Frasnian cyrtospiriferids directly overlying the middle Devonian (Ma and Zong, 2010). Reef builders (such as corals and stromatoporoids) were severely influenced, causing the demise of coral-stromatoporoid bioherms and the proliferation of microbial bioherms and stromatoporoid biostromes (Wu et al., 2010). Meanwhile, $\delta^{13}\text{C}_{\text{carb}}$ value increases with an amplitude of 2.5–3‰ around the G-F boundary, indicating the onset of the collapse of Devonian metazoan reef systems and major perturbations of marine carbon cycle during this time interval, which are correlated with the Frasnian event.

3.4.5 The F-F mass extinction event

The F-F event represents one of the ‘big five’ mass extinctions of the Phanerozoic (Sepkoski, 1996; McGhee et al., 2013), causing significant dropdown of marine biodiversity, major changes in the community structure, and collapse of the largest reef ecosystems (Copper, 1994; Walliser, 1996). This event includes two episodes, corresponding to the lower and upper Kellwasser events, respectively. It is closely related to the global changes of climate, sea-level and marine redox conditions (Joachimski et al., 2009).

The lower Kellwasser event occurs in the lower part of the upper *Pa. rhenana* zone, and is poorly studied in South China. It can only be recognized by the major positive shifts of carbon, oxygen, and strontium isotopic records in the transitional facies and deep-water basins (e.g., the Fuhe,

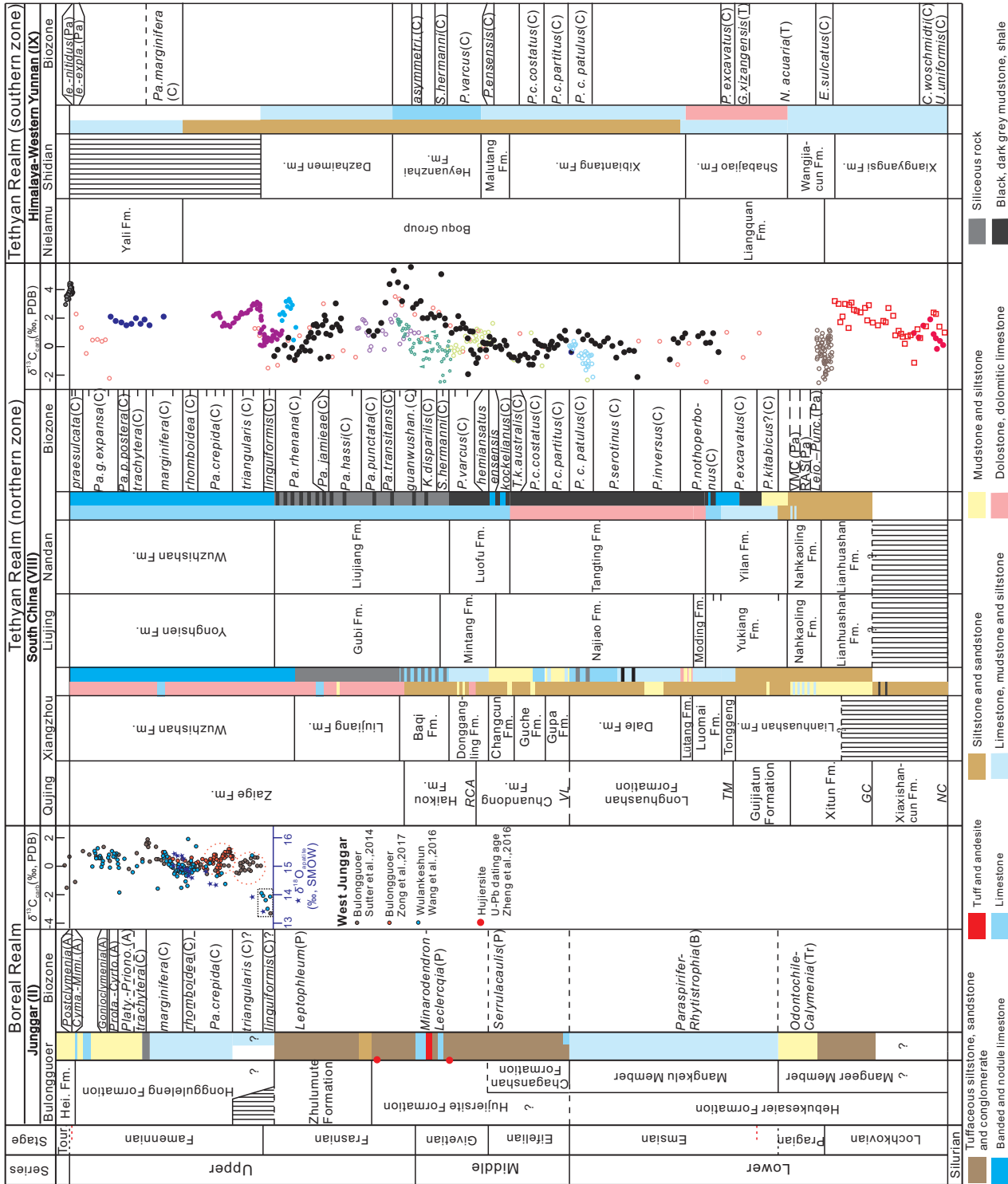


Figure 4 Devonian stratigraphic correlation between major palaeobiogeography realms in China. The carbon isotopic records encircled by red dashed lines are actually from equivalent intervals, plotted here based on the authors' different viewpoints.

Dongcun, and Baisha sections of Guilin, and the Nantong section of Wuxuan), indicating abundant burial of organic carbon, global climate cooling and increased terrestrial inputs during this time (Chen et al., 2005; Xu et al., 2012; Huang, 2015).

The upper Kellwasser event occurs around the Frasnian-Famennian boundary (the *Pa. linguiformis* zone and lower *Pa. triangularis* zone), and represents the main episode of the F-F mass extinction. It had a major impact on the benthic fauna groups, such as brachiopods, corals and ostracods in the shallow marine ecosystem (Chen and Ma, 2004; Liao, 2004; Wang, 2004). There existed obvious discrepancies among different fossil groups in terms of extinction pattern and extinction mechanism (Ma et al., 2016). In deep-water facies, the demise of Frasnian conodonts are estimated to have lasted less than 200 kyr (Huang and Gong, 2016). Major fluctuations of carbon, oxygen, and sulfur isotopic records in South China have been reported in previous researches, and have great significance for revealing marine geochemical cycle perturbation during this critical time interval (Chen et al., 2013; Huang, 2015).

3.4.6 The Hangenberg event

The Hangenberg event occurred in the middle and upper *S. praesulcata* zones near the Devonian-Carboniferous boundary, within a short time span of about 100–300 kyr (Myrow et al., 2013). Recent studies revealed that this event was at least as severe as the F-F extinction event, and represents one of the largest mass extinctions in the Phanerozoic (Becker et al., 2012; Kaiser et al., 2016). In South China, the biotic and environmental responses to the Hangenberg event were basically identical to other regions around the world, including: (1) the main extinction level is in the middle *S. praesulcata* zone, marked by widespread black shale in deep-water facies, and sedimentary gap or lithological changes in shallow-water facies, indicating a sea-level fall event during this time (Qie et al., 2015); (2) marine communities were severely affected, among which the stromatoporoids, chitinozoans, placoderms, Leperditicopida and Palmatolepids became extinct, only a few cymaclymeniids survived the main extinction levels, and Devonian-type corals, trilobites, and acritarch, foraminifera and vertebrate animals experienced great biodiversity loss, interrupting the biotic recovery in the aftermath of the F-F mass extinction; (3) the survivors became extinction in the upper *S. praesulcata* zone, which is consistent with the global sea-level rise following the latest Devonian glaciation, changeover of terrestrial floras, and the appearance of Carboniferous-type organisms; (4) carbon and nitrogen isotopic records in South China indicate major marine geochemical cycle perturbations (Liu et al., 2016).

3.5 Cyclostratigraphy and radiometric age

Cyclostratigraphy is a powerful tool in high-resolution stratigraphic subdivision and correlation. As for the Cenozoic strata, continuous, high-resolution (20–100 kyr) astronomical time scale has been established by identifying the Milankovitch cycles in sedimentary records, and tuning these cycles to the astronomical solutions (ATS, Hinnov, 2004). As for the Paleozoic strata, astronomically calibrated floating time scales with time resolution of 400 kyr could be provided by the interpretation of cyclic variations in the sedimentary records, and in combination of radiometric age, enable us to precisely determine the timing and durations of major biotic, climatic and environmental events, and to improve the accuracy and resolution of geologic time scale (De Vleeschouwe et al., 2012, 2013; Da Silva et al., 2016).

Studies on Devonian cyclostratigraphy of China started early in the 90s of last century, Bai et al. (1994) and Bai (1995) indicated that the 100 kyr period in chemical element abundances and ratios recovered from the Devonian sediments in South China, was formed in response to the orbital perturbations of eccentricity, the duration of one Devonian conodont zone is between 0.05 Myr and 1.0 Myr, and the Frasnian Stage lasted about 5 Myr. Gong et al. (2005) recognized hierarchically organized laminae, bundles, bundlesets and superbundlesets in the upper Givetian to lower Famennian in Guangxi, which were considered to be consistent with a sub-Milankovitch (8–10 kyr), precession or obliquity (1.67 kyr or 3.33 kyr), eccentricity (100 kyr) and long eccentricity (400 kyr) cyclothem, respectively. The duration of 12 standard conodont zones of Frasnian and early Famennian have been elaborated, and the Frasnian Stage has been estimated to have lasted 4.3 Myr. However, in GTS 2012, the duration of the Frasnian is 9.5 Ma, indicating that previous studies on Devonian cyclostratigraphy of China need further improvement. In order to testify the orbital signatures illustrated by diverse climate proxies, time-series analysis, cyclostratigraphic correlation among different regions, and calibration by accurate radiometric age are needed.

In China, isotope geochronology studies on Devonian stratigraphy is extremely limited, and only one valid radiometric age was reported from the Devonian-Carboniferous boundary interval in South China. Liu et al. (2012) conducted SHRIMP U-Pb analyses on the zircons extracted from the Hangenberg event horizon in the Daposhang section, Guizhou province, yielding 20 concordant data that form a cluster with a $^{206}\text{Pb}/^{238}\text{U}$ concordia age of 359.6 ± 1.9 Ma. Combined with previous biostratigraphy and sequence stratigraphy results, the age of the DCB at Daposhang, South China is estimated at 359.58 Ma, which has been adopted by the Stratigraphic Chart of China (2014) (Figure 3).

4. Correlation of the Devonian sequences of China

On the basis of paleogeography configuration, geotectonic properties of the sedimentary basins and paleobiological features, the Devonian of China can be subdivided into 9 stratigraphic regions (Figure 5), including Altai-Hinggan (I), Junggar (II), Tarim (III), North China (IV), Qilian-Kunlun (V), Qinlin (VI), Qiangtang-Three Rivers (VII), South China (VIII) and Himalaya-western Yunnan (IX). Stratigraphic correlation between different stratigraphic regions of China is mainly based on biostratigraphy of pelagic fossils, especially the conodont, graptolite and tentaculite. However, since biostratigraphic framework has not been well established in the other regions, high-resolution stratigraphic correlation with the standard sequences in South China is unachievable at present (Figure 4).

Devonian was a period of great tectonic activity, climatic fluctuations, and sea-level variations, and global provincialism of marine biota was evident. According to tectonic, climatic and biotic features, Zhao (1988) recognized three realms on a global scale, i.e., the Boreal, Tethyan (including northern and southern zone) and Malvinocaffric Realms. During this time, China was composed of multiple, separated blocks that were located in the northern and southern margins of the Paleotethys Ocean, and moving northward in general. The Altai-Hinggan Region belonged to the south margin of the Siberia, and the Junggar Region was part of the Kazakhstan Plate, both regions developed combination of terrestrial sediments, shallow-marine siliciclastic and carbonate sediments, deep-water flysch and volcanic sediments in tectonically active settings, i.e., active continental margin or island arc zones. The Altai-Hinggan and Junggar regions belonged to the Boreal Realm, and fossil associations are similar to Siberia and Kazakhstan. The lower Devonian of the Junggar Region has yielded a diverse fossil assemblage consisting of trilobite *Odontochile* and brachiopod *Leptaenopyxis* and *Paraspirifer* with rare rugose corals, except in the Mangkelu Member of the Hebukesai Formation, abundant and diverse rugose corals were found, but distinct from the time-equivalent assemblages in South China (Liao and Cai, 1987; Hou et al., 1988). Early Devonian rugose corals, such as *Siphonophrentis* and *Schlotheimophyllum*, developed well in the eastern Inner Mongolia and Hinggan regions, characterized by small solitary, no-dissepiment and thickening of peripheral sterozone, which may indicate temperate climate. Due to the lack of systematic studies on the biostratigraphy of pelagic fossil, the precise locations for the base of the Lochkovian, Pragian and Emsian stages in the Boreal Realm cannot be located. According to lycopid plant association, most previous studies suggested the Hujiersite Formation of the Junggar Region spans late Eifelian to Givetian. Due to fault-bound outcrops and lack of index fossils,

the age of the Hujiersite Formation and its contact relation with the underlying Hebukesai Formation and Chaganshan Formation (or Hefeng Formation) remain unclear (Xiao et al., 1991; Wang et al., 2004) (Figure 4). Spores *Acinosporites lindlarensis* and *Rotaspora* sp. were recently extracted from the plants beds of the Hujiersite Formation by Xu et al. (2014), and enable to date these beds as from late Emsian to Eifelian in age. Zheng et al. (2016) conducted U-Pb ICP-MS analyses of detrital zircons from the upper part of the Hujiersite Formation, which gave a maximum depositional age of 380 Ma and indicated that this formation could range up to lower Frasnian (Figure 4). In recent years, studies on the lithostratigraphy, conodont, ammonoids and brachiopod biostratigraphy, carbon isotope stratigraphy and event stratigraphy have been completed in the Famennian Hongguleleng Formation, enable the establishment of a high-resolution integrative stratigraphic framework for the Famennian of Junggar (Suttner et al., 2014; Carmichael et al., 2014, 2016; Zong et al., 2015, 2016, 2017; Wang, 2016; Ma et al., 2017b) (Figure 4). Nevertheless, the accurate locations of the Frasnian-Famennian and Devonian-Carboniferous boundaries remain controversial. Combined with the conodont biostratigraphy, Suttner et al. (2014) and Wang (2016) suggested that the major positive shift of $\delta^{13}\text{C}$ values in the basal Hongguleleng Formation, with an amplitude of $>3\%$, is consistent with the global carbon isotope curve, and indicate F-F boundary is located at the base of the Hongguleleng Formation. However, Zong et al. (2017) proposed that no typical Frasnian conodonts have been found in western Junggar, and the major $\delta^{13}\text{C}$ shift was mainly caused by diagenetic alternation around the lithological boundary and the actual pattern of $\delta^{13}\text{C}$ is consistent with the global isotope records in the *Pa. crepida* zone-*Pa. rhomboidea* zone of Famennian, indicating the basal Famennian is missing in this area (Figure 4). In the lower part of the Heishantou Formation (equivalent to the upper part of the Hongguleleng Formation defined by Chinese scholar), Carmichael et al. (2016) detected a marine anoxic event using petrologic and geochemical proxies, and considered it to represent the Hangenberg event, while Zong et al. (2016) suggested that the Hangenberg extinction event occurs at the base of the Heishantou Formation, characterized by the demise of brachiopod *Austrospirifer?* sp. assemblage and the appearance of *Syringothyris-Spirifer* assemblage.

During the Devonian, the Himalaya-western Yunnan Region, included in the southern zone of the Tethyan Realm, was located in the northern margin of the Indian Plate, and developed shallow-water siliciclastic and carbonate facies in marginal sea environment (Figure 4). In the Mount Everest region of Tibet, the Liangquan Formation yields a diverse assemblage consisting of graptolite *N. himalayensis*, *U. thomasi*, tentaculite *Nowakia acuaria*, *Guerichina xizangensis* etc., and can be correlated with the Pragian and

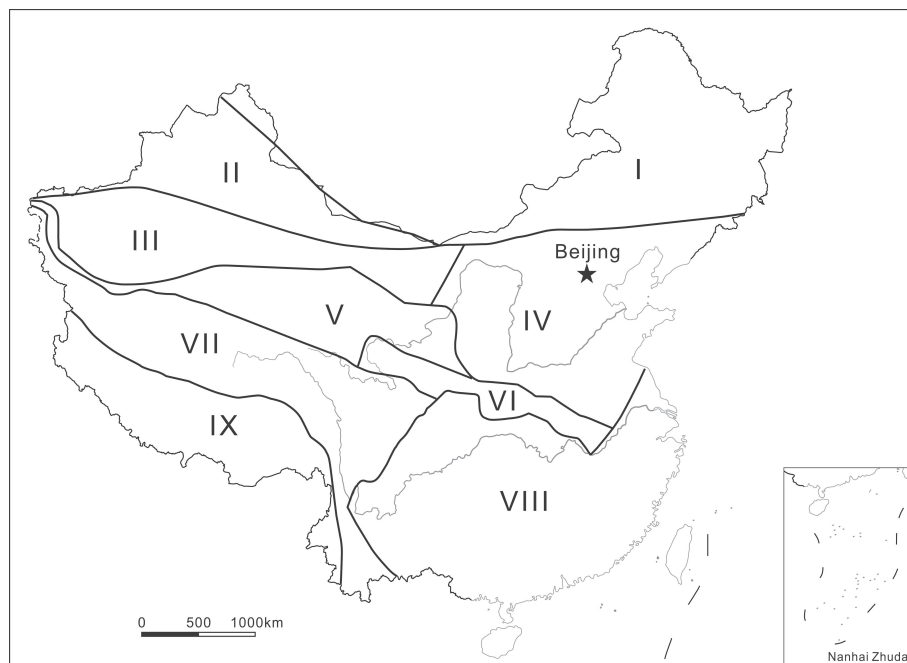


Figure 5 Tectonic-stratigraphic regions of the Devonian in China. I. Altai-Hinggan; II. Junggar; III. Tarim; IV. North China; V. Qilian-Kunlu; VI. Qinlin; VII. Qiangtang-Three Rivers; VIII. South China; IX. Himalaya-western Yunnan.

lower Emsian in Yulin-Qinzhou, South China; the overlying Boqu Group is mainly composed of medium- to coarse-grained quartzose sandstone with rare fossils, and cannot be further subdivided and well correlated with its counterparts; the Yali Formation contains index fossils of the spore LE, LN and VP zones, indicating the DCB is located in the lower part of the Yali Formation (Figure 4). In Baoshan and Shidian, western Yunnan, graptolite *U. cf. uniformis* and conodont “*C. woschmidt*” are recorded in the Xiangyangsi Formation, and the SDB may be situated in the basal part of the Xiangyangsi Formation; the overlying Wangjiacun, Shabajiao and Xibiantang formations contain graptolites, tentaculites and conodonts that could be used to make precise correlation with the standard sequences in South China, and the lower-middle Devonian boundary is located in the upper part of the Xibiantang Formation (Figure 4); Middle and upper Devonian are represented by a diverse assemblage consisting of abundant rugose and tabulate corals, brachiopods, and trilobites, which is quite different from the time equivalent assemblages in South China, e.g., the typical brachiopod genera in northern zone of the Tethyan Realm, such as *Stringocephalus*, have not been found. Standard conodont biostratigraphic sequences of the Malutang and Heyuanzhai formations have been established by Dong and Wang (2006), which enable precise stratigraphic subdivision and correlation of the middle Devonian in western Yunnan and the assignment of the top Heyuanzhai Formation to the Frasnian (Figure 4).

All the other stratigraphic regions of China belonged to the northern zone of the Tethyan Realm, with little attention

being paid to the biostratigraphy and chronostratigraphy except for the South China Region. The Tarim, North China and Qilian-Kulun plates were thought to be adjacent to each other during the Devonian, and in most areas, the lower and middle Devonian did not develop due to the exposure and erosion, and the upper Devonian is mainly composed of terrestrial red conglomerate, sandy conglomerate and sandstone yielding plants, spores and fish fragments; marine strata are restricted in the north and southwest margins of the Tarim Plate, characterized by mixed siliciclastic and carbonate platform facies and benthic communities. Brachiopod *Stringocephalus*, which are widespread in the middle Devonian of South China, were also reported in the Tuogemaiti and Saeraming formations of southern Tianshan. Based on palynological assemblages, the Qizilafu and Donghetang formations in Tarim Basin have been assigned to Famennian and middle Famennian (Ouyang et al., 2017), respectively, and the DCB in the Bachu Formation is located within the lower mudstone Member (Zhu et al., 2000). In the Qinlin and Qiangtang-Three Rivers regions, the biota show high similarity with South China, e.g., in Diebu and Changdu, brachiopod assemblages could be well correlated with the standard sequences in South China (Hou et al., 1988). 14 coral assemblage zones and 17 brachiopod assemblage zones were recognized in Diebu, Qinlin, which enable precise stratigraphic subdivision. However, the biostratigraphic sequences of pelagic fossils have been poorly studied and the recognition of key chronostratigraphic boundaries need further improvement. Zhao et al. (2011) presented detailed $\delta^{13}\text{C}_{\text{org}}$ records at the Putonggou and Yanglugou sections,

Qinlin and recognized a major positive shift of $\delta^{13}\text{C}_{\text{org}}$ in the Silurian-Devonian transitional intervals, together with previous conodont evidence, precisely located the SDB in the successions.

5. Conclusions and implications

Based on well-studied biostratigraphy, carbon isotopic stratigraphy and event stratigraphy of Devonian in South China and adjacent areas, this paper provides an updated Devonian integrative stratigraphy framework of China, facilitating precise stratigraphic subdivision and correlation in different paleogeographic settings. Nevertheless, there are still many deficiencies concerning Devonian timescale of China, including: (1) few studies have been conducted on the astronomical cyclostratigraphy and radioactive isotope dating, leading to lower-resolution time scale; (2) the Chinese regional stages lack strict boundary definition, and need further subdivision; (3) no continuous, complete Devonian carbon, oxygen and sulfur isotopic curves have been reported in China, and previous geochemical data are mainly restricted within the Frasnian-Famennian boundary intervals; (4) except for the South China Region, integrated stratigraphy studies of the Devonian System in other stratigraphic regions are very limited.

At present, the main tasks for the SDS include revising the GSSPs for the base of the Emsian Stage and Devonian-Carboniferous boundary, subdividing Devonian substages, and improving correlation between the deep- and shallow-water facies, and between marine and terrestrial strata, respectively. Meanwhile, IGCP 652 (2017–2020) aims to establish high-resolution astronomical time scale using integrated biostratigraphy, cyclostratigraphy and radiometric dating means, and to determine the timing and durations of the important Paleozoic events recorded in the sedimentary records.

In South China, nearly complete deep-water sequences of Emsian to Famennian were reported in the Nandan type facies, and provide excellent sedimentary records for the establishment of high-resolution astronomical time scale of Devonian; the transitional and paralic facies are widely distributed in South China, and characterized by diverse and abundant fossil records, which are in favor of precise correlation between marine and terrestrial strata, and between global standard and Chinese regional stages. For the DCB intervals, numerous studies have been conducted on the bio-, litho-, isotopic stratigraphy and event stratigraphy in South China, making it an ideal place to revise the Devonian-Carboniferous boundary GSSP.

Acknowledgements *We are grateful to two anonymous reviewers for their constructive comments and suggestions. This work was supported by*

the Strategic Priority Research Program (B) of Chinese Academy of Sciences (Grant Nos. XDB26000000, XDB18000000), the National Natural Science Foundation of China (Grant Nos. 41290260, 41772004, 41772012), the Special Program for Basic Research of the Ministry of Science and Technology, China (Grant No. 2013FY111000) and the State Key Laboratory of Palaeobiology and Stratigraphy, Nanjing Institute of Geology and Palaeontology, CAS.

References

- Algeo T J, Berner R A, Maynard J B, Scheckler S E. 1995. Late Devonian oceanic anoxic events and biotic crises: "Rooted" in the Evolution of vascular land plants? *GSA Today*, 5: 64–66
- Aretz M. 2010. Report of the Joint Devonian-Carboniferous Boundary GSSP Reappraisal Task Group. *Newsl Carbonif Stratigr*, 28: 26–30
- Bai S L. 1995. Milankovitch cyclicity and time scale of the Middle and Upper Devonian. *Int Geol Rev*, 37: 1109–1114
- Bai S L, Bai Z Q, Ma X P, Wang D R, Sun Y L. 1994. Devonian Events and Biostratigraphy of South China. Beijing: Peking University Press. 303
- Bai S L, Jin S Y, Ning Z S. 1982. Devonian Biostratigraphy of Guangxi and Adjacent Area (in Chinese). Beijing: Peking University Press. 203
- Baliński A, Sun Y L. 2016. *Cyrtinoides Yudina* and *Rzhonsnitskaya*, 1985, an aberrant Middle Devonian ambocoeliid brachiopod genus from China. *Palaeoworld*, 25: 632–638
- Becker R T. 2009. SDS Annual Report to ICS 2008. *Subcomm Devonian Stratigr Newsl*, 24: 2–7
- Becker R T, Aboussalam Z S. 2011. Emsian chronostratigraphy-preliminary new data and a review of the Tafilalt (SE Morocco). *Subcomm Devonian Stratigr Newsl*, 26: 33–43
- Becker R T, Gradstein F M, Hammer O. 2012. The Devonian Period. In: Gradstein F M, Ogg J G, Schmitz M D, Ogg G M, eds. *The Geologic Time Scale 2012, Volume 2*. Amsterdam: Elsevier. 559–601
- Buggisch W, Joachimski M M. 2006. Carbon isotope stratigraphy of the Devonian of Central and Southern Europe. *Palaeogeogr Palaeoclimatol Palaeoecol*, 240: 68–88
- Bureau of Geology and Mineral Resources of Guangxi. 1985. Regional Geology of Guangxi Zhuang Autonomous Region (in Chinese). Beijing: Geological Publishing House. 1–853
- Cai C Y. 2000. Nonmarine Devonian. In: Nanjing Institute of Geology and Palaeontology, Chinese Academy of Sciences, ed. *Stratigraphical Studies in China (1979–1999)* (in Chinese). Hefei: University of Science and Technology of China Press. 95–127
- Cai C Y, Wang Y. 1995. Devonian floras. In: Li X X, ed. *Fossil Floras of China through the Geological Ages*. Guangzhou: Guangdong Science and Technology Press, 28–77
- Carls P, Gandl A J. 1969. Stratigraphie und Conodonten des Unter-Devons der Östlichen Iberischen Ketten (NE-Spanien). *Neues Jahrbuch für Geologie und Paläontologie Abhandlungen*, 132: 155–218
- Carls P, Slavik L, Valenzuela-Ríos J I. 2007. Revisions of conodont biostratigraphy across the Silurian-Devonian boundary. *Bull Geosci*, 82: 145–164
- Carls P, Slavik L, Valenzuela-Ríos J I. 2008. Comments on the GSSP for the basal Emsian stage boundary: The need for its redefinition. *Bull Geosci*, 83: 383–390
- Carmichael S K, Waters J A, Batchelor C J, Coleman D M, Suttner T J, Kido E, Moore L M, Chadimová L. 2016. Climate instability and tipping points in the Late Devonian: Detection of the Hangenberg Event in an open oceanic island arc in the Central Asian Orogenic Belt. *Gondwana Res*, 32: 213–231
- Carmichael S K, Waters J A, Suttner T J, Kido E, DeReuil A A. 2014. A new model for the Kellwasser Anoxia Events (Late Devonian): Shallow water anoxia in an open oceanic setting in the Central Asian Orogenic Belt. *Palaeogeogr Palaeoclimatol Palaeoecol*, 399: 394–403
- Chang J Q, Bai Z Q, Sun Y L, Peng Y B, Qin S J, Shen B. 2017. High resolution bio- and chemostratigraphic framework at the Frasnian-Fa-

- mennian boundary: Implications for regional stratigraphic correlation between different sedimentary facies in South China. *Palaeogeogr Palaeoclimatol Palaeoecol*, DOI: 10.1016/j.palaeo. 2017.05.019
- Chen D, Qing H, Li R. 2005. The Late Devonian Frasnian-Famennian (F/F) biotic crisis: Insights from C_{org} - C_{org} and $^{87}Sr/^{86}Sr$ isotopic systematics. *Earth Planet Sci Lett*, 235: 151–166
- Chen D, Wang J, Racki G, Li H, Wang C, Ma X, Whalen M T. 2013. Large sulphur isotopic perturbations and oceanic changes during the Frasnian-Famennian transition of the Late Devonian. *J Geol Soc*, 170: 465–476
- Chen X, Quan Q Q. 1992. Earliest Devonian graptolites from Ximeng, southwestern Yunnan, China. *Australasian J Palaeontol*, 16: 181–187
- Chen X, Ni Y, Lenz A C, Zhang L, Chen Z, Tang L, Jin J. 2015. Early Devonian graptolites from the Qinzhou-Yulin region, southeast Guangxi, China. *Can J Earth Sci*, 52: 1000–1013
- Chen X Q, Ma X P. 2004. Late Devonian brachiopod mass extinction of South China. In: Rong J Y, Fang Z J, eds. *Mass Extinction and Recovery—Evidences from the Palaeozoic and Triassic of South China* (in Chinese). Hefei: University of Science and Technology of China Press. 317–356
- Chlupáč I, Kukal Z. 1977. The boundary stratotype at Klonek. *The Silurian-Devonian Boundary*. IUGS Ser A, 5: 96–109
- Chlupáč I, Oliver W A. 1989. Decision on the Lochkovian-Pragian Boundary stratotype (Lower Devonian). *Episodes*, 12: 109–114
- Copper P. 1994. Ancient reef ecosystem expansion and collapse. *Coral Reefs*, 13: 3–11
- Cui B Q, Lu C W, Yang S Q. 1993. Strontium and carbon isotopes and sea level fluctuation of Devonian in Longmen Mountain region (in Chinese). *J Chengdu Coll Geol*, 20: 1–8
- Da Silva A C, Hladil J, Chadimová L, Slavik L, Hilgen F J, Bábek O, Dekkers M J. 2016. Refining the Early Devonian time scale using Milankovitch cyclicity in Lochkovian-Pragian sediments (Prague Synform, Czech Republic). *Earth Planet Sci Lett*, 455: 125–139
- Davidson T. 1853. On some fossil brachiopods, of the Devonian age, from China. *Quarterly J Geol Soc London*, 9: 353–359
- De Koninck L. G. 1846. Notice sur deux especes de Brachiopodes du terrain Paleozoique de la Chine. *Bulletin de l'Academie Royale des Sciences Lettres et Beaux Arts, de Belgique*, 13: 415–426
- De Vleeschouwer D, Rakociński M, Racki G, Bond D P G, Sobieñ K, Claeys P. 2013. The astronomical rhythm of Late-Devonian climate change (Kowala section, Holy Cross Mountains, Poland). *Earth Planet Sci Lett*, 365: 25–37
- De Vleeschouwer D, Whalen M T, (Jed) Day J E, Claeys P. 2012. Cyclostratigraphic calibration of the Frasnian (Late Devonian) time scale (western Alberta, Canada). *Geol Soc Am Bull*, 124: 928–942
- Dong Z Z, Wang W. 2006. The Cambrian-Triassic Conodont Faunas in Yunnan, China (in Chinese). Kunming: Yunnan Science and Technology Press. 347
- Feng J L. 1930. Some problems in the Geology of Kwangtung and Kwangsi (in Chinese). *Bull Geol Soc China*, 9: 127–133
- Foster G L, Royer D L, Lunt D J. 2017. Future climate forcing potentially without precedent in the last 420 million years. *Nat Commun*, 8: 14845
- Gao L D. 1990. Miospore zones in the Devonian-Carboniferous boundary beds in Hunan and their stratigraphical significance (in Chinese). *Geol Rev*, 36: 58–68
- Garcia-Alcalde, J. 1997. North Gondwanan Emsian events. *Episodes*, 20: 241–246
- Geng L Y, Wang Y, Cai X Y, Tang P. 2000. Chitinozoan biostratigraphy in China. In: *Palynoforas and Palynomorphs of China*. Hefei: Press of University of Science and Technology of China. 209–241
- Gerrienne P, Meyer-Berthaud B, Yang N, Steemans P, Li C S. 2014. Planatophyton gen. nov., a late Early or Middle Devonian euphylllophyte from Xinjiang, North-West China. *Rev Palaeobot Palynol*, 208: 55–64
- Goddéris Y, Donnadiou Y, Le Hir G, Lefebvre V, Nardin E. 2014. The role of palaeogeography in the Phanerozoic history of atmospheric CO₂ and climate. *Earth Sci Rev*, 128: 122–138
- Gong Y. 2005. The Upper Devonian orbital cyclostratigraphy and numerical dating conodont zones from Guangxi, South China. *Sci China Ser D-Earth Sci*, 48: 32–41
- Grabau A W. 1931. Devonian Brachiopoda of China, I: Devonian Brachiopoda from Yunnan and other districts in South China. *Palaeontol Sin Ser B*, 3: 1–538
- Gradstein F M, Ogg J G, Schmitz M D, Ogg G M. 2012. *The Geological Time Scale 2012, Volume 2*. Amsterdam: Elsevier. 1144
- Groos-Uffenorde H, Lethiers F, Blumenstengel H. 2000. Ostracodes and Devonian stratigraphy. *Cour Forsch Inst Senckenberg*, 220: 99–111
- Guo W. 2017. Lower Emsian (Lower Devonian) conodont biostratigraphy and brachiopod faunal replacement of South China (in Chinese). Doctoral Dissertation. Beijing: Peking University. 1–114
- Guo W, Sun Y L, Baliński A. 2015. Parallel evolution of jugal structures in Devonian athyridide brachiopods. *Palaeontology*, 58: 171–182
- Hao S G, Xue J Z. 2013. *The Early Devonian Posongchong Flora of Yunnan—A Contribution to an Understanding of the Evolution and Early Diversification of Vascular Plants*. Beijing: Science Press. 366
- Hinnov L A. 2004. Earth's orbital parameters and cycle stratigraphy. In: Gradstein F M, Ogg J G, Smith A G, eds. *A Geologic Time Scale 2004*. Cambridge: Cambridge University Press, 55–62
- Hou H F. 1978. Devonian strata in South China. In: *Institute of Geology, Mineral Resources, Chinese Academy of Geological Sciences, ed. Symposium on the Devonian Strata of South China* (in Chinese). Beijing: Geological Publishing House. 214–230
- Hou H F. 1981. Devonian brachiopod biostratigraphy of China. *Geol Mag*, 118: 185–192
- Hou H F, Chen X Q, Rong J Y, Ma X P, Zhang Y, Xu H K, Su Y Z, Xian S Y, Zong P. 2017. Devonian brachiopod genera on type species of China. In: Rong J Y, Jin Y G, Shen S Z, Zhan R B, eds. *Phanerozoic Brachiopod Genera of China*. Beijing: Science Press. 343–557
- Hou H F, Ji Q, Wu X H, Xiong J F, Wang S T, Gao L D, Sheng H B, Wei J Y, Tener S. 1985. *Muhua Sections of Devonian-Carboniferous Boundary Beds* (in Chinese). Beijing: Geological Publishing House. 226
- Hou H F, Ma X P. 2005. Devonian GSSPs and division of the Devonian System in South China (in Chinese). *J Stratigr*, 29: 154–159
- Hou H F, Wang S T. 1988. *Stratigraphy of China, No. 7: The Devonian System of China* (in Chinese). Beijing: Geological Publishing House. 348
- House M R. 2002. Strength, timing, setting and cause of mid-Palaeozoic extinctions. *Palaeogeogr Palaeoclimatol Palaeoecol*, 181: 5–25
- Huang C. 2015. The peculiarities and causes of the Devonian F-F event: Evidences from high-resolution conodont biostratigraphy and chemostratigraphy in South China (in Chinese). Doctoral Dissertation. Wuhan: China University of Geosciences. 1–146
- Huang C, Gong Y. 2016. Timing and patterns of the Frasnian-Famennian event: Evidences from high-resolution conodont biostratigraphy and event stratigraphy at the Yangdi section, Guangxi, South China. *Palaeogeogr Palaeoclimatol Palaeoecol*, 448: 317–338
- Huang S J. 1997. A study on carbon and strontium isotopes of late Palaeozoic carbonate rocks in the upper Yangtze Platform (in Chinese). *Acta Geol Sin*, 71: 45–53
- Huang S J, Shi H, Zhang Y, Wu W H, Shen W C. 2002. Global correlation of strontium isotope evolution curve of Devonian in Longmen Mountain and dating marine sediments (in Chinese). *Prog Nat Sci*, 12: 945–951
- Husson J M, Schoene B, Blüher S, Maloof A C. 2016. Chemostratigraphic and U-Pb geochronologic constraints on carbon cycling across the Silurian-Devonian boundary. *Earth Planet Sci Lett*, 436: 108–120
- Ji Q, Wei J Y, Wang Z J, Wang S T, Sheng H B, Wang H D, Hou J P, Xiang L W, Feng R L, Fu G M. 1989. *The Dapoushang Section—An Excellent Section for the Devonian-Carboniferous Boundary Stratotype in China*. Beijing: Science Press. 1165
- Ji Q, Ziegler W. 1993. The Lali section—An excellent reference section for Upper Devonian in South China. *Cour Forsch Inst Senckenberg*, 157: 1–183
- Jin S Y, Shen A J, Chen Z L, Lu J M, Wei M, Wang Y Q, Xie F. 2005. *Mixed Biostratigraphy of Devonian in Wenshan, Yunnan*. Beijing: Petroleum Industry Press. 195

- Joachimski M M, Breisig S, Buggisch W, Talent J A, Mawson R, Gereke M, Morrow J R, Day J, Weddige K. 2009. Devonian climate and reef evolution: Insights from oxygen isotopes in apatite. *Earth Planet Sci Lett*, 284: 599–609
- Joachimski M M, Pancost R D, Freeman K H, Ostertag-Henning C, Buggisch W. 2002. Carbon isotope geochemistry of the Frasnian-Famennian transition. *Palaeogeogr Palaeoclimatol Palaeoecol*, 181: 91–109
- Kaiser S I. 2005. Mass extinctions, climatic and oceanographic changes at the Devonian-Carboniferous boundary. Doctorial Dissertation. Bochum: Ruhr-University. 1–156
- Kaiser S I, Aretz M, Becker R T. 2016. The global Hangenberg Crisis (Devonian-Carboniferous transition): Review of a first-order mass extinction. *Geol Soc London Spec Publ*, 423: 387–437
- Kaiser S I, Corradini C. 2011. The early Siphonodellids (Conodonta, Late Devonian-Early Carboniferous): Overview and taxonomic state. *Neues Jahrbuch für Geologie und Paläontologie Abhandlungen*, 261: 19–35
- Königshof P, Silva A C D, Sutter T J, Kido E, Waters J, Carmichael S K, Jansen U, Pas D, Spassov S. 2016. Shallow-water facies setting around the Kačák Event: A multidisciplinary approach. In: Becker R T, Königshof P, Brett C E, eds. *Devonian climate, sea level and evolutionary events*. *Geol Soc London Spec Publ*, 423: 171–199
- Kuang G D, Zhao T M, Tao Y B. 1989. The Standard Devonian Section of China—Liujiing section of Guangxi (in Chinese). Wuhan: China University of Geosciences Press. 154
- Liao W H. 2004. Coral recovery from the Frasnian-Famennian mass extinction event in South China. In: Rong J Y, Fang Z J, eds. *Mass Extinction and Recovery—Evidences from the Palaeozoic and Triassic of South China* (in Chinese). Hefei: University of Science and Technology of China Press. 259–280
- Liao W H. 2006. Biodiversity of Devonian rugose corals from South China. In: Rong J Y, Fang Z J, Zhou Z H, Zhan R B, Wang X D, Yuan X L, eds. *Originations, Radiations and Biodiversity Changes—evidences from the Chinese Fossil Record* (in Chinese). Beijing: Science Press. 417–428
- Liao W H. 2015. Two major faunal turnover events of middle Devonian corals in South China (in Chinese). *Acta Palaeont Sin*, 54: 305–315
- Liao W H, Cai T C. 1987. Sequence of Devonian rugose coral assemblages from northern Xinjiang (in Chinese). *Acta Palaeont Sin*, 26: 689–707
- Liao W H, Ruan Y P. 2003. Devonian Biostratigraphy of China. In: Zhang W T, Chen P J, Palmer A R, eds. *Biostratigraphy of China*. Beijing: Science Press. 237–279
- Liu J, Bai Z Q. 2009. Chemostratigraphy of Mg, Ca, Na, Sr, $\delta^{13}\text{C}$, $\delta^{18}\text{O}$ in middle Devonian strata of Liujiing section, Guangxi (in Chinese). *Geophys Geochem Expl*, 33: 417–423
- Liu J, Qie W, Algeo T J, Yao L, Huang J, Luo G. 2016. Changes in marine nitrogen fixation and denitrification rates during the end-Devonian mass extinction. *Palaeogeogr Palaeoclimatol Palaeoecol*, 448: 195–206
- Liu Y Q, Ji Q, Kuang H W, Jiang X J, Xu H, Peng N. 2012. U-Pb zircon age, sedimentary facies, and sequence stratigraphy of the Devonian-Carboniferous boundary, Daposhang Section, Guizhou, China. *Palaeoworld*, 21: 100–107
- Lu J F, Qie W K, Chen X Q. 2016. Pragian and lower Emsian (Lower Devonian) conodonts from Liujiing, Guangxi, South China. *Australasian J Palaeontol*, 40: 275–296
- Ma X, Gong Y, Chen D, Racki G, Chen X, Liao W. 2016. The Late Devonian Frasnian-Famennian Event in South China—Patterns and causes of extinctions, sea level changes, and isotope variations. *Palaeogeogr Palaeoclimatol Palaeoecol*, 448: 224–244
- Ma X P, Liao W H, Wang D M. 2009. The Devonian System of China, with a discussion on sea-level change in South China. In: Königshof P, ed. *Devonian Change: Case Studies in Palaeogeography and Palaeoecology*. *Geol Soc London Spec Publ*, 314: 241–262
- Ma X P, Wang C Y, Racki G, Racka M. 2008. Facies and geochemistry across the Early-Middle Frasnian transition (Late Devonian) on South China carbonate shelf: Comparison with the Polish reference succession. *Palaeogeogr Palaeoclimatol Palaeoecol*, 269: 130–151
- Ma X P, Wang H H, Zhang M Q. 2017a. Devonian event succession and sea level change in South China —With Early and Middle Devonian carbon and oxygen isotopic data. *Subcomm Devonian Stratigr Newsl*, 32: 17–24
- Ma X, Zhang M, Zong P, Zhang Y, Lü D. 2017b. Temporal and spatial distribution of the Late Devonian (Famennian) strata in the north-western border of the Junggar Basin, Xinjiang, Northwestern China. *Acta Geol Sin*, 91: 1413–1437
- Ma X P, Zhang Y B, Zhang M Q. 2014. Lithologic and biotic aspects of major Devonian events in South China. *Subcomm Devonian Stratigr Newsl*, 29: 21–33
- Ma X P, Zong P. 2010. Middle and Late Devonian brachiopod assemblages, sea level change and paleogeography of Hunan, China. *Sci China Earth Sci*, 53: 1849–1863
- Manda Š, Frýda J. 2010. Silurian-Devonian boundary events and their influence on cephalopod evolution: Evolutionary significance of cephalopod egg size during mass extinctions. *Bull Geosci*, 85: 513–540
- McArthur J M, Howarth R J, Shields G A. 2012. Strontium Isotope Stratigraphy. In: Gradstein F M, Ogg J G, Schmitz M D, Ogg G M, eds. *The Geologic Time Scale 2012, Volume 1*. Amsterdam: Elsevier. 127–144
- McGhee Jr. G R, Clapham M E, Sheehan P M, Bottjer D J, Droser M L. 2013. A new ecological-severity ranking of major Phanerozoic biodiversity crises. *Palaeogeogr Palaeoclimatol Palaeoecol*, 370: 260–270
- Murphy M A. 2005. Pragian conodont zonal classification in Nevada, western North America. *Rev Esp Palaeontol*, 20: 177–206
- Mu E Z, Chen X, Ni Y N, Mu D C, Yuan J L, Wei R Y, Yao Z G, Yin B A, Shi W J, Zhang J D. 1988. The Silurian and Devonian of Qinzhou and Yulin, Guangxi (in Chinese). *J Stratigr*, 12: 241–254
- Mu E Z, Ni Y N. 1975. The Silurian and Devonian graptolites from the Jolmolungma Region (in Chinese). In: *Rept Sci Invest Jolmolungma Region (Palaeont Fasc 1)*. Beijing: Science Press. 1–27
- Myrow P M, Ramezani J, Hanson A E, Bowring S A, Racki G, Rakociński M. 2013. High-precision U-Pb age and duration of the latest Devonian (Famennian) Hangenberg event, and its implications. *Terra Nova*, 26: 222–229
- NCSC (National Commission on Stratigraphy of China). 2014. *The Stratigraphic Chart of China (2014)* (in Chinese). Beijing: Geological Publishing House. 1
- Nie T, Guo W, Sun Y L, Shen B, Yin B A, Tang Z H, Li Y K, Huang X L, Mai C. 2016. Age and distribution of the Late Devonian brachiopod genus *Dzieduszyckia* Siemiradzki, 1909 in southern China. *Palaeoworld*, 25: 600–615
- Ogg J G, Ogg G M, Gradstein F M. 2016. *A Concise Geologic Time Scale*. Amsterdam: Elsevier. 232
- Ouyang S, Lu L C, Zhu H C, Liu F. 2017. *The Late Paleozoic Spores and Pollen of China* (in Chinese). Hefei: University of Science and Technology of China Press. 1092
- Paproth E, Feist R, Flajs G. 1991. Decision on the Devonian-Carboniferous boundary stratotype. *Episodes*, 14: 331–336
- Percival L M E, Davies J H F L, Schaltegger U, De Vleeschouwer D, Da Silva A C, Föllmi K B. 2018. Precisely dating the Frasnian-Famennian boundary: Implications for the cause of the Late Devonian mass extinction. *Sci Rep*, 8: 9578
- Pribyl A. 1940. Graptolitová fauna českého středního Ludlow (svrchní eř). *Vestník státního geologického Ústavu*, 16: 63–73
- Qie W, Liu J, Chen J, Wang X, Mii H, Zhang X, Huang X, Yao L, Algeo T J, Luo G. 2015. Local overprints on the global carbonate $\delta^{13}\text{C}$ signal in Devonian-Carboniferous boundary successions of South China. *Palaeogeogr Palaeoclimatol Palaeoecol*, 418: 290–303
- Qie W, Wang X D, Zhang X, Ji W, Grossman E L, Huang X, Liu J, Luo G. 2016. Latest Devonian to earliest Carboniferous conodont and carbon isotope stratigraphy of a shallow-water sequence in South China. *Geol J*, 51: 915–935
- Racki G. 2005. Toward understanding Late Devonian global events: Few answers, many questions. In: Over O J, Morrow J R, Wignall P B, eds. *Understanding Late Devonian and Permian-Triassic Biotic and Climatic Events, Towards an Integrated Approach*. Amsterdam: Elsevier. 5–36
- Ruan Y P. 1979. Devonian ammonoid zonation of China (in Chinese). *Acta*

- Stratigr Sin, 3: 134–137
- Ruan Y P, Mu D C. 1989. Devonian tentaculitoids from Guangxi (in Chinese). *Mem Nanjing Inst Geol Palaeont, Acad Sin*, 26: 1–238
- Saltzman M R, Thomas E. 2012. Carbon Isotope Stratigraphy. In: Gradstein F M, Ogg J G, Schmitz M D, Ogg G M, eds. *The Geologic Time Scale 2012*, Volume 1. Amsterdam: Elsevier. 207–232
- Sedgwick A, Murchison, R I. 1839. Stratification of the older stratified deposits of Devonshire and Cornwall. *Philos Mag*, 3: 241–260
- Sepkoski Jr. J J. 1996. Patterns of Phanerozoic extinction: A perspective from global data bases. In: Walliser O H, ed. *Global Events and Event Stratigraphy in the Phanerozoic*. Berlin: Springer-Verlag. 35–51
- Slavik L, Brett C E. 2016. Minutes of the Ghent Business Meeting. *Subcomm Devonian Stratigr Newsl*, 31: 21–25
- Slavik L, Carls P, Hladil J, Koptikova L. 2012. Subdivision of the Lochkovian Stage based on conodont faunas from the stratotype area (Prague Synform, Czech Republic). *Geol J*, 47: 616–631
- Spalletta C, Perri M C, Over D J, Corradini C. 2017. Famennian (Upper Devonian) conodont zonation: revised global standard. *Bull Geosci*, 92: 31–57
- Song J J, Gong Y M. 2015. Progresses and Prospects of Palaeozoic ostracod study (in Chinese). *Acta Paleontol Sin*, 54: 404–424
- Stephens N P, Sumner D Y. 2003. Late Devonian carbon isotope stratigraphy and sea level fluctuations, Canning Basin, Western Australia. *Palaeogeogr Palaeoclimatol Palaeoecol*, 191: 203–219
- Sun Y L. 1992. Fossil brachiopods from Eifelian-Givetian boundary bed of Liujing section, Guangxi, China (in Chinese). *Acta Palaeont Sin*, 31: 708–723
- Sun Y L, Bai S L. 1995. Lower range of *Stringocephalus*. *Newsl Stratigr*, 32: 73–77
- Sun Y L, Boucot A J. 1999. Ontogeny of *Stringocephalus gubiensis* and the origin of *Stringocephalus*. *J Paleontol*, 73: 860–871
- Sutter T J, Kido E, Chen X, Mawson R, Waters J A, Frýda J, Mathieson D, Molloy P D, Pickett J, Webster G D, Frýdová B. 2014. Stratigraphy and facies development of the marine Late Devonian near the Boulongour Reservoir, northwest Xinjiang, China. *J Asian Earth Sci*, 80: 101–118
- Tan Z X. 1987. Brachiopod. In: *Regional Geological Surveying Party, Bureau of Geology and Mineral Resources of Hunan Province, ed. The Late Devonian and Early Carboniferous Strata and Palaeobiocoenosis of Hunan* (in Chinese). Beijing: Geological Publishing House. 111–133
- Tien C C. 1938. The Devonian of China (in Chinese). *Geol Rev*, 13: 203–210
- van Geldern R, Joachimski M M, Day J, Jansen U, Alvarez F, Yolkin E A, Ma X P. 2006. Carbon, oxygen and strontium isotope records of Devonian brachiopod shell calcite. *Palaeogeogr Palaeoclimatol Palaeoecol*, 240: 47–67
- Walliser O H. 1996. Global events in the Devonian and Carboniferous. In: Walliser O H, ed. *Global Events and Event Stratigraphy in the Phanerozoic*. Berlin: Springer-Verlag. 225–250
- Wang C Y. 1981. Lower Devonian conodonts from the Xiaputonggou Formation at Zoige, NW Sichuan (in Chinese). *Bull Xi'an Inst Geol M R Chinese Acad Geol Sci*, No. 3: 77–84
- Wang C Y. 1989. Devonian conodonts of Guangxi (in Chinese). *Mem Nanjing Inst Geol Palaeont Acad Sin*, 25: 1–212
- Wang C Y. 2000. Devonian. In: *Nanjing Institute of Geology and Palaeontology, Chinese Academy of Sciences, ed. Stratigraphical Studies in China (1979–1999)* (in Chinese). Hefei: University of Science and Technology of China Press. 73–94
- Wang C Y. 2018. *Devonian Conodonts of China* (in Chinese). Beijing: Science Press. in press
- Wang C Y, Chen B, Kuang G D. 2016. Lower Devonian conodonts from the Nagaoling Formation of the Dashatian section near Nanning, Guangxi, South China (in Chinese). *Acta Micropalaeont Sin*, 33: 420–435
- Wang C Y, Peng S C. 2017. Promoting the international chronostratigraphic chart in China (in Chinese). *J Stratigr*, 41: 216–220
- Wang C Y, Wang P, Yang G H, Xie W. 2009. Restudy on the Silurian conodont biostratigraphy of the Baizitian section in Yanbian County, Sichuan (in Chinese). *J Stratigr*, 33: 302–317
- Wang C Y, Ziegler W. 1983. Conodonten aus Tibet. *Neues Jahrbuch für Geologie und Paläontologie. Monatshefte*, (2): 69–79
- Wang C S, Li Z H, Peng Z Q, Wang B Z, Zhang G T. 2014. The carbon isotope variation and its responses to sea level changes during the late Early Devonian period in Guizhou and Guangxi (in Chinese). *Geol China*, 41: 2039–2047
- Wang D M, Hao S G, Liu Z F. 2002. Researches on plants from the Lower Devonian Xujiachong Formation in the Qujing district, eastern Yunnan. *Acta Geol Sin*, 76: 393–407
- Wang D R, Bai Z Q. 2002. Chemostratigraphic characters of the middle-upper Devonian boundary in Guangxi, South China (in Chinese). *J Stratigr*, 26: 50–54
- Wang P. 2006. Lower Devonian conodonts of the Bateabao area in Darha Muning'an joint Banner, Inner Mongolia (in Chinese). *Acta Micropalaeont Sin*, 23: 199–234
- Wang S Q. 1983. Late Devonian pelagic ostracod sequences in Luofu region of Guangxi (in Chinese). *Chin Sci Bull*, 4: 234–236
- Wang S Q. 1986. Devonian Rhomboentomozoinae (ostracoda) from Guangxi (in Chinese). *Acta Palaeont Sin*, 25: 155–168
- Wang S Q. 2004. Mass extinction of late Devonian Leperditicopids (ostracoda). In: Rong J Y, Fang Z J, eds. *Mass Extinction and Recovery—Evidences from the Palaeozoic and Triassic of South China* (in Chinese). Hefei: University of Science and Technology of China Press. 357–366
- Wang S Q. 2009. Paleozoic Entomozoacea and Leperditicopida (ostracoda). In: *Fossil Ostracoda of China, Vol. 3* (in Chinese). Hefei: University of Science and Technology of China Press. 251
- Wang S Q, Peng J L. 2005. Biostratigraphical significance of the Devonian *Sinoleperditini* (Ostracoda). *Sci China Ser D-Earth Sci*, 48: 1666–1671
- Wang X F. 1988. Graptolite. In: Hou H F, Wang S T, eds. *Stratigraphy of China, No. 7: The Devonian System of China* (in Chinese). Beijing: Geological Publishing House. 236–239
- Wang X F, Chen X H et al. 2004. Division and Correlation of Each Geologic Period in China (in Chinese). Beijing: Geological Publishing House. 596
- Wang Y, Berry C M, Hao S G, Xu H H, Fu Q. 2007. The Xichong flora of Yunnan, China: Diversity in late Middle Devonian plant assemblages. *Geol J*, 42: 339–350
- Wang Y, Hao S G, Fu Q, Xu H H, Wang D M. 2006. Biodiversity of early land vascular plants in the Silurian and Devonian of China. In: Rong J Y, Fang Z J, Zhou Z H, Zhan R B, Wang X D, Yuan X L, eds. *Originations, Radiations and Biodiversity Changes—Evidences from the Chinese Fossil Record* (in Chinese). Beijing: Science Press. 383–398
- Wang Y, Xu H H. 2005. *Sublepidodendron grabaui* comb. nov., a lycopsid from the Upper Devonian of China. *Bot J Linn Soc*, 149: 299–311
- Wang Y, Yu C M, Wang C Y, Ruan Y P. 1981. Subdivision of the Devonian of China (in Chinese). *Sci Bull*, 26: 230–232
- Wang Y, Yu C M. 1962. *The Devonian of China* (in Chinese). Beijing: Science Press. 140
- Wang Y, Yu C M, Wu Q. 1974. Advances in the Devonian biostratigraphy of South China (in Chinese). *Mem Nanjing Inst Geol Paleont Acad Sin*, 6: 1–45
- Wang Z H. 2016. Late Devonian conodont biostratigraphy and carbon and oxygen isotopic composition in western Junggar, NW China (in Chinese). *Doctoral Dissertation*. Wuhan: China University of Geosciences. 1–137
- Wu Y, Yan C X. 1980. The lower and middle Devonian of Debao, Guangxi (in Chinese). *J Stratigr*, 201–208
- Wu Y B, Gong Y M, Zhang L J, Feng Q. 2010. Evolution and controlling factors of the Devonian bioreefs in South China (in Chinese). *J Palaeogeogr*, 12: 253–267
- Xia F S. 1997. Conodonts from the Arpishmebulaq Formation (late Lochkovian) of eastern South Tianshan and their significance (in Chinese). *Acta Palaeont Sin*, 36(Suppl), 77–96
- Xian S Y. 1998. The silicified brachiopod fossils from the base of the Mintang Formation (middle Devonian) in Liujing, Guangxi (in Chi-

- nese). *Litho Paleogeogr*, 18: 28–47
- Xiao S L, Wu S Z, Wang B Y, Wang S R, Hou H F. 1991. Some new advances in study on Devonian in Sarburti region of West Junggar, Xinjiang (in Chinese). *Xinjiang Geol Sci*, 3: 1–9
- Xu B, Gu Z, Wang C, Hao Q, Han J, Liu Q, Wang L, Lu Y. 2012. Carbon isotopic evidence for the associations of decreasing atmospheric CO₂ level with the Frasnian-Famennian mass extinction. *J Geophys Res*, 117: G01032
- Xu H K. 1977. Early-Middle Devonian plicanopliids from Nandan of Guangxi (in Chinese). *Acta Palaeont Sin*, 16: 59–70
- Xu H K. 1979. Brachiopods from the Tangxiang Formation (Devonian) in Nandan of Guangxi (in Chinese). *Acta Palaeont Sin*, 18: 362–380
- Xu H H, Berry C M, Wang Y. 2011. Morphological study on the Devonian zosterophyll *Serrulacaulis Hueber* and Banks: New materials and emendation. *Palaeoworld*, 20: 322–331
- Xu H H, Jiang Q, Zhang X L, Wang Y, Fu Q, Feng J. 2015. On the middle Devonian Hujiersite flora from West Junggar, Xinjiang, China, its characteristics, age, palaeoenvironment and palaeophytogeographical significances (in Chinese). *Acta Palaeont Sin*, 54: 230–239
- Xu H H, Marshall J E A, Wang Y, Zhu H C, Berry C M, Wellman C H. 2014. Devonian spores from an intra-oceanic volcanic arc, West Junggar (Xinjiang, China) and the palaeogeographical significance of the associated fossil plant beds. *Rev Palaeobot Palynol*, 206: 10–22
- Xu H H, Wang Y. 2008. The palaeogeographical significance of specimens attributed to *Protolepidodendron scharyanum* Krejčí (Lycopsida) from the Middle Devonian of North Xinjiang, China. *Geol Mag*, 145: 295–299
- Xue J. 2009. Two zosterophyll plants from the Lower Devonian (Lochkovian) Xitun Formation of Northeastern Yunnan, China. *Acta Geol Sin*, 83: 504–512
- Yoh S S. 1938. Beitrage zur Kenntnis des marinen oberen Unterdevons und unter Mitteldevons Sudchina. *Bull Geol Soc China*, 18: 67–73
- Yolkin E A, Kim A I, Weddige K, Talent J A, House M R. 1997. Definition of the Pragian/Emsian Stage boundary. *Episodes*, 20: 235–240
- Yolkin E A., Weddige K, Izokh N G, Erina M. 1994. New Emsian conodont zonation (Lower Devonian). *Cour Forsch Inst Senckenberg*, 168: 139–157
- Yu C M. 1988. Devonian-Carboniferous Boundary in Nanbiancun, Guilin, China: Aspects and Records. Beijing: Science Press. 379
- Yu C M, Qie W K, Lu J F. 2018. Emsian (Early Devonian) Yujiang Event in South China. *Palaeoworld*, 27: 53–65
- Zhao X W. 1988. Devonian. In: Yin H F et al., eds. *Paleobiogeography of China* (in Chinese). Wuhan: China University of Geosciences Press. 134–150
- Zhao W, Jia G, Zhu M, Zhu Y. 2015. Geochemical and palaeontological evidence for the definition of the Silurian/Devonian boundary in the Changwantang Section, Guangxi Province, China. *Estonian J Earth Sci*, 64: 110–114
- Zhao W, Wang N, Zhu M, Mann U, Herten U, Lücke A. 2011. Geochemical stratigraphy and microvertebrate assemblage sequences across the Silurian/Devonian Transition in South China. *Acta Geol Sin*, 85: 340–353
- Zheng D, Xu H, Wang J, Feng C, Zhang H, Chang S C. 2016. Geochronologic age constraints on the Middle Devonian Hujiersite flora of Xinjiang, NW China. *Palaeogeogr Palaeoclimatol Palaeoecol*, 463: 230–237
- Zhong K, Wu Y, Yin B A, Liang Y L, Yao Z G, Peng J L. 1992. Devonian of Guangxi (in Chinese). Wuhan: China University of Geosciences. 384
- Zhu M, Wang N Z, Wang J Q. 2000. Devonian macro- and microvertebrate assemblages of China. *Cour Forsch Inst Senckenberg*, 223: 361–372
- Zhu H C, Zhang S B, Luo H, Gao Q Q, Wang Q F, Huang Z B, Tang P, Du P D. 2000. New advances in the study of the Devonian-Carboniferous Boundary in the Tarim Basin (in Chinese). *J Stratigr*, 24(Suppl): 371–372
- Ziegler W, Klapper G. 1985. Stages of the Devonian System. *Episodes*, 8: 104–109
- Zong P, Becker R T, Ma X. 2015. Upper Devonian (Famennian) and Lower Carboniferous (Tournaesian) ammonoids from western Junggar, Xinjiang, northwestern China—Stratigraphy, taxonomy and palaeobiogeography. *Palaeobio Palaeoenviron*, 95: 159–202
- Zong P, Ma X, Xue J, Jin X. 2016. Comparative study of Late Devonian (Famennian) brachiopod assemblages, sea level changes, and geoevents in northwestern and southern China. *Palaeogeogr Palaeoclimatol Palaeoecol*, 448: 298–316
- Zong P, Ma X P, Zhang M Q, Zhang Y B, Lü D. 2017. Comparative study of Famennian carbon isotope characteristics of Junggar, Xinjiang and Central Hunan, South China (in Chinese). *Acta Sci Natur Univ Peking*, 53: 843–861

(Responsible editor: Shuzhong SHEN)